

Calculation of radiation losses in cylinder symmetric high pressure discharges by means of a digital computer

Citation for published version (APA):

Andriessen, F. J., Boerman, W., & Holtz, I. F. E. M. (1973). *Calculation of radiation losses in cylinder symmetric high pressure discharges by means of a digital computer*. (EUT report. E, Fac. of Electrical Engineering; Vol. 73-E-38). Technische Hogeschool Eindhoven.

Document status and date:

Published: 01/01/1973

Document Version:

Publisher's PDF, also known as Version of Record (includes final page, issue and volume numbers)

Please check the document version of this publication:

- A submitted manuscript is the version of the article upon submission and before peer-review. There can be important differences between the submitted version and the official published version of record. People interested in the research are advised to contact the author for the final version of the publication, or visit the DOI to the publisher's website.
- The final author version and the galley proof are versions of the publication after peer review.
- The final published version features the final layout of the paper including the volume, issue and page numbers.

[Link to publication](#)

General rights

Copyright and moral rights for the publications made accessible in the public portal are retained by the authors and/or other copyright owners and it is a condition of accessing publications that users recognise and abide by the legal requirements associated with these rights.

- Users may download and print one copy of any publication from the public portal for the purpose of private study or research.
- You may not further distribute the material or use it for any profit-making activity or commercial gain
- You may freely distribute the URL identifying the publication in the public portal.

If the publication is distributed under the terms of Article 25fa of the Dutch Copyright Act, indicated by the "Taverne" license above, please follow below link for the End User Agreement:

www.tue.nl/taverne

Take down policy

If you believe that this document breaches copyright please contact us at:

openaccess@tue.nl

providing details and we will investigate your claim.

th

e

Calculation of radiation losses in cylinder symmetric
high pressure discharges by means of a digital computer

F. J. Andriessen

W. Boerman

I. F. E. M. Holtz

TECHNISCHE HOGESCHOOL EINDHOVEN
NEDERLAND
AFDELING DER ELEKTROTECHNIEK
GROEP HOGE SPANNINGEN EN HOGE STROMEN

EINDHOVEN UNIVERSITY OF TECHNOLOGY
THE NETHERLANDS
DEPARTMENT OF ELECTRICAL ENGINEERING
GROUP HIGH VOLTAGES AND HIGH CURRENTS

Calculation of radiation losses in cylinder symmetric
high pressure discharges by means of a digital computer

F.J. Andriessen

W. Boerman

I.F.E.M. Holtz

augustus 1973

TH-Report 73 - E - 38

ISBN 90 6144 038 6

<u>Contents</u>	<u>Page</u>
I. The radiative transfer equation	- 1 -
I-1. Introduction	- 1 -
I-2. Solution of the radiative transfer equation	- 1 -
II. Emission and absorption of radiation in a high pressure discharge	- 4 -
II-1. Free-free absorption	- 4 -
II-2. Bound-free absorption and emission	- 5 -
II-3. Line absorption and emission coefficients	- 9 -
III. Absorption and emission coefficients for the NI continuum and NI, NII lines	-12 -
III-1. The NI continuum	-12 -
III-2. The NI and NII lines	-16 -
IV. Description of the computer programmes for the calculation of the radiative balance in a cylinder symmetric discharge	-18 -
IV-1. Introduction	-18 -
IV-2. The exponential integral B(g)	-19 -
IV-3. Calculation of the absorption and emission coefficient	-22 -
IV-4. Calculation of the contribution of a spectral line to the radiative balance in the axis of the discharge	-24 -
IV-5. Calculation of the distribution of a spectral line to the radiative balance in points out of the axis of a discharge	-27 -
IV-6. Calculation of the contribution of the bound-free continuum ($h\nu > I$) to the radiative balance in a cylindrically symmetric discharge	-30 -
V. Radiative losses in discharges in a forced gas flow	-31 -
V-1. Temperature distributions	-31 -
V-2. The radiative balance	-32 -
Literature	-37 -
Appendices I, II, III and IV.	

1. The radiative transfer equation.

1-1. Introduction.

Investigations carried out on wall-stabilized electric arcs in nitrogen and argon [1, 2, 3] have shown that radiative energy transfer is no longer negligible when the central temperature rises above about 12,000 °K. In particular, the energy transfer by means of ultra-violet radiation ($\lambda < 2000 \text{ \AA}$), which is subject to reabsorption in the discharge, plays an important part in the total energy balance of the discharge.

In the general case, where reabsorption of emitted radiation in a discharge which is in L.T.E. is not negligible, the calculation of the radiative energy transfer is based on the stationary radiative transfer equation which is given by [4, 5]:

$$\vec{\Omega} \text{ grad } I_{\nu} = \alpha'_{\nu} [I_{\nu p} - I_{\nu}] \quad (1)$$

in which the unit vector $\vec{\Omega}$ indicates the propagation direction of the radiation, I_{ν} is the intensity of the radiation with frequency ν , $I_{\nu p}$ is the intensity of the black body radiation and α'_{ν} the (spectral) absorption coefficient, corrected for the induced emission. ($\alpha'_{\nu} = \alpha_{\nu} \{1 - \exp(-h\nu/kT)\}$).

1-2. Solution of the radiative transfer equation.

The contribution made by radiation from all directions to the total radiative energy balance at a certain point, is obtained by integrating equation (1) over the total solid angle 4π .

With $\vec{\Omega} \text{ grad } I_{\nu} = \text{div} (\vec{\Omega} I_{\nu})$, ($\text{div } \vec{\Omega} \equiv 0$) this gives:

$$\int_{4\pi} \text{div} (\vec{\Omega} I_{\nu}) d\Omega = \text{div} \int_{4\pi} \vec{\Omega} I_{\nu} d\Omega = \int_{4\pi} \epsilon_{\nu} d\Omega - \int_{4\pi} \alpha'_{\nu} I_{\nu} d\Omega \quad (2)$$

in which $d\Omega$ is an element of the solid angle around a unit vector $\vec{\Omega}$ and $\epsilon_{\nu} = \alpha'_{\nu} I_{\nu p}$ is the (spectral) emission coefficient.

The term $\int_{4\pi} \vec{\Omega} I_{\nu} d\Omega$ represents the spectral flux vector \vec{q}_{ν} .

The two terms on the right-hand side of equation (2) represent respectively the total emitted and the total absorbed radiation energy per unit volume, time and frequency; these are indicated by e_{ν} and a_{ν} respectively.

Obviously (2) can now be written as:

$$\operatorname{div} \vec{q}_{\nu} = e_{\nu} - a_{\nu} = u_{\nu} \quad (3)$$

Here the term u_{ν} is the balance between the emitted and absorbed radiation energy per unit volume, time and frequency.

Assuming that the coefficients ϵ_{ν} and α_{ν} are isotropic, it can be shown that at a point $r = 0$ the terms \vec{q}_{ν} , a_{ν} and e_{ν} are given by [2]:

$$\vec{q}_{\nu}(r = 0) = \int \int \int \vec{\Omega} \epsilon_{\nu}(\vec{r}) \exp\left(-\int_0^r \alpha_{\nu}' d\rho\right) \frac{1}{r^2} dV \quad (4)$$

$$a_{\nu}(r = 0) = \alpha_{\nu}'(r = 0) \int \int \int \epsilon_{\nu}(\vec{r}) \exp\left(-\int_0^r \alpha_{\nu}' d\rho\right) \frac{1}{r^2} dV \quad (5)$$

$$e_{\nu}(r = 0) = 4\pi\epsilon_{\nu}(r = 0) \quad (6)$$

One can distinguish two extremes:

- a) Where the absorption coefficient α_{ν}' is very large, so that the mean free path $\bar{\lambda}_{\nu}$ of the photons ($\bar{\lambda}_{\nu} = 1/\alpha_{\nu}'$) is so small that at a given point ($r = 0$) the only radiation arriving will be that from the immediate neighbourhood of that point, for which ϵ_{ν} is practically constant. Then from equations (4, 5, 6) with $\epsilon_{\nu}(\vec{r}) = \alpha_{\nu}'(r = 0)$ follows:

$$\vec{q}_{\nu} = 0; \quad a_{\nu} = 4\pi\epsilon_{\nu}; \quad u_{\nu} = e_{\nu} - a_{\nu} = 0 \quad (7)$$

(equilibrium radiation)

- b) For very small values of α_{ν}' the situation may occur in which in a medium of limited extent the absorption per unit volume a_{ν} is negligibly small with respect to the emission per unit volume e_{ν} .

In determining the radiative energy transfer, a first approximation will be given by:

$$\operatorname{div} \vec{q}_v = e_v = u_v \quad (8)$$

(optically thin radiation)

If the value of α'_v lies between the two extremes mentioned above, the calculation of \vec{q}_v and a_v at a given point will require integration over the total volume of the medium emitting the radiation. The calculation of the total radiative energy flux $\vec{q}(\int \vec{q}_v dv)$; the total emission $e(\int e_v dv)$ and absorption $a(\int a_v dv)$ of radiative energy per unit volume and time will also require integration over the frequency range of the emitted radiation.

In the special case of cylinder symmetry, we can simplify (6) and (5) as follows [2]:

$$e_v(r_A) = e_v(T_{r_A}) = 4\pi \epsilon_v(T_{r_A}) \quad (9)$$

$$a_v(r_A) = 4\alpha'_v(r_A) \int_0^R \epsilon_v(r_Q) r_Q \int_0^\pi \frac{B(g)}{\sqrt{r_A^2 + r_Q^2 - 2r_A r_Q \cos\phi}} d\phi dr_Q \quad (10)$$

in which $B(g)$ is given by: $B(g) = \int_0^{\pi/2} \exp(-g/\cos\theta) d\theta$ (11)

with $g/\cos\theta$, the optical thickness, given by:

$$\frac{g}{\cos\theta} \int_Q^A \alpha'_v dl = \frac{1}{\cos\theta} \int_P^A \alpha'_v ds \quad (12)$$

The variables are shown in figure 1.

The expression for α_v in the centre of the discharge ($r = 0$), can be considerably simplified because, as a result of the symmetry, the integration over the angle ϕ in (10) can be carried out directly reading:

$$\alpha_v(r_A = 0) = \alpha'_v(r_A = 0) \int_0^R 4\pi \epsilon_v(r_Q) B(g) dr_Q \quad (13)$$

with $g = \int_0^{r_Q} \alpha'_v(r) dr$

Despite the cylinder-symmetry, the calculation of $a(r)$ involves a great deal of work, which can be carried out properly using a digital computer.

However, it is essential for the calculation of $(a)r$ that the coefficients ϵ_v and α_v^i from equations (10) and (13) are known as a function of position in the medium. The following two sections will deal with this in more detail.

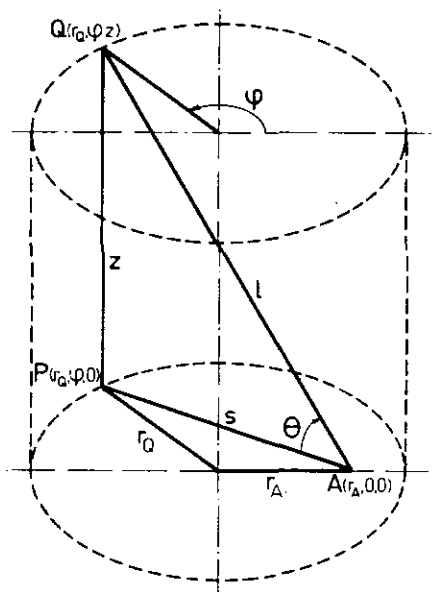


Fig. 1. Co-ordinates of the source Point Q and the observation point A.

II. Emission and absorption of radiation in a high pressure discharge.

II-1. Free-free absorption.

As early as 1923 Kramers [6] derived the following relationship for the free-free absorption coefficient for one ion with charge $Z.e$ and one absorbing electron, with velocity v , per unit volume:

$$\alpha_v = \frac{4 \pi}{3\sqrt{3}} \frac{Z^2}{hcm_e^2} \frac{e^6}{(4\pi\epsilon_0)^3 v} \frac{1}{v^3} \quad (14)$$

where:

h = Planck's constant ($6.6256 \cdot 10^{-34}$ J sec)

e = elementary charge ($1.60210 \cdot 10^{-19}$ C)

m_e = electron rest mass ($9.1091 \cdot 10^{-31}$ kg)

c = speed of light in vacuum ($2.9979 \cdot 10^8$ m sec $^{-1}$)

ϵ_0 = vacuum permittivity ($100/36\pi \cdot 10^{-11}$ F/m)

With n_i ions per unit volume and dn_e electrons in the velocity interval

between v and $v + dv$, assuming L.T.E., integration over the Maxwellian velocity distribution of the electrons gives the following expression for the free-free absorption coefficient [7]:

$$\alpha_{\nu_{ff}} = g_{ff} \frac{16\pi^2}{3\sqrt{3}} \frac{Z^2 e^6}{hc(2\pi m_e)^{3/2} (4\pi\epsilon_0)^3} \frac{n_e n_i}{(kT)^{1/2}} \frac{1}{\nu^3} \quad (15)$$

where k is Boltzmann's constant and g_{ff} is the Gaunt factor. The Gaunt factor takes into account the deviations from Kramers' theory. An expression for this factor is given by Griem [8]. The value of g_{ff} is usually about unity.

11-2. Bound-free absorption and emission.

If the distribution of atoms among the excited states is a Boltzmann distribution, then for hydrogen, the bound-free absorption coefficient is found as follows [9]:

Kramers' formula (14) is applied to all states with the same principal quantum number n , and a summation over the lower excited levels and an integration over the upper excited levels is then carried out. Unsöld [10] extended the expression which holds for hydrogen to complex atoms. The structural peculiarities of complex atoms were taken into account by introducing an effective nuclear charge Z^* and a factor γ/U_A . γ is the ratio of the number of sub-levels in a complex atom for the given principal and orbital quantum numbers n and ℓ , to the analogous quantity for the hydrogen atom and U_A is the partition function of the complex atom.

The quantity Z^* is given by Unsöld as:

$$Z^{*2} = n^2 \frac{I_A - I_{n,\ell}}{I_H} \quad (16)$$

where $I_{n,\ell}$ corresponds to the actual energy of the level of the complex atom with the given quantum numbers n and ℓ . I_A and I_H are the ionization energies of the complex atom and hydrogen atom respectively. Hence the following expressions for the bound-free absorption coefficients were obtained [9, 11]:

$$\alpha_{\nu_{bf}} = \frac{16\pi^2}{3\sqrt{3}} \frac{e^6}{(4\pi\epsilon_0)^3} \frac{Z^{*2} \gamma kT n_A}{U_A h^4 c^3 \nu^3} \exp(-I_A/kT) [\exp(h\nu/kT)-1] \quad (17)$$

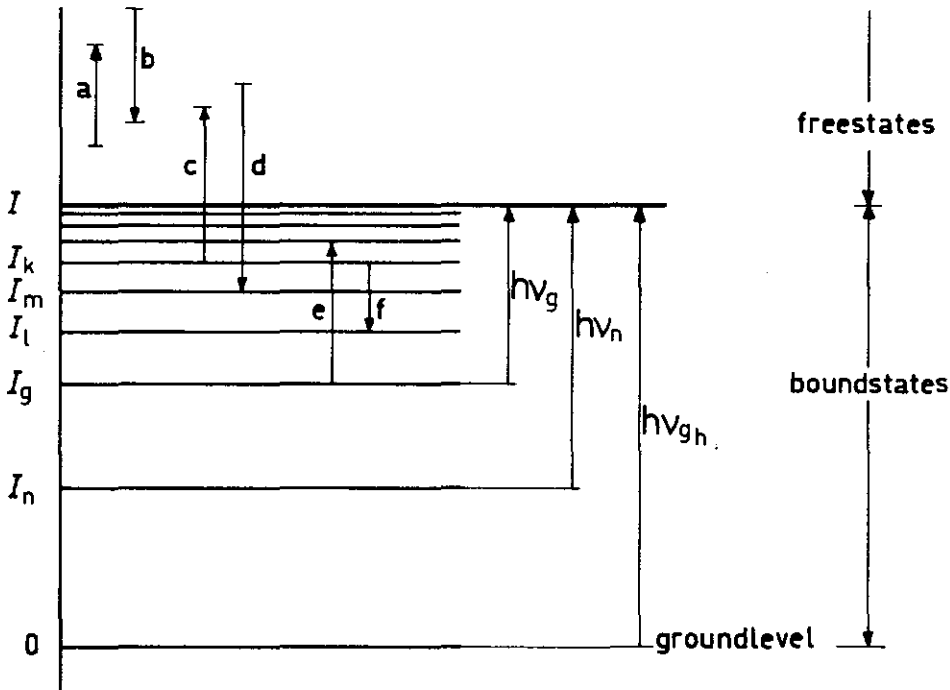
$$\nu \leq \nu_g$$

$$\alpha_{\nu_{bf}} = \frac{16\pi^2}{3\sqrt{3}} \frac{e^6}{(4\pi\epsilon_0)^3} \frac{Z^{*2} \gamma kT n_A}{U_A h^4 c \nu^3} \exp(-I_A/kT) [\exp(h\nu_g/kT)-1] \quad (18)$$

$$\nu > \nu_g$$

where n_A is the particle density of the complex atoms per unit volume and ν_g is the frequency limit of the close lying terms given by:

$$\nu_g = (I - I_g) / h \quad (\text{see figure 2})$$



- | | |
|---------------------------|-------------------------|
| a) free-free absorption | b) free-free emission |
| c) bound-free absorption | d) free-bound emission |
| e) bound-bound absorption | f) bound-bound emission |

Fig. 2. Schematic diagram of energy states and transitions for atom, ion or electron.

The absorption coefficient for the whole continuum is obtained from the expressions for $\alpha_{\nu_{bf}}$ by the addition of the free-free absorption coefficient $\alpha_{\nu_{ff}}$ found from equation (15). With the help of the Saha equation, the product $n_i n_e$ in equation (15) can be expressed in terms of the number of atoms n_A per unit volume, giving for the continuum absorption coefficient for complex atoms the following expressions [9, 11]:

$$\alpha_{\nu} = \frac{16\pi^2}{3\sqrt{3}} \frac{e^6}{(4\pi\epsilon_0)^3} \frac{\gamma Z^{*2} kT n_A}{U_A h^4 c \nu^3} \exp [(h\nu - I_A)/kT] \quad *) \quad (19)$$

$$\nu \leq \nu_g$$

$$\alpha_{\nu} = \frac{16\pi^2}{3\sqrt{3}} \frac{e^6}{(4\pi\epsilon_0)^3} \frac{\gamma Z^{*2} kT n_A}{U_A h^4 c \nu^3} \exp [(h\nu_g - I_A)/kT] \quad (20)$$

$$\nu > \nu_g$$

When L.T.E. applies, the relationship between the emission coefficient ϵ_{ν} and the absorption coefficient α_{ν} is given by Kirchhoff's law:

$$\epsilon_{\nu} = \alpha_{\nu} I_{\nu p} [1 - \exp(-h\nu/kT)] = \alpha'_{\nu} I_{\nu p} \quad (21)$$

in which the term $\{1 - \exp(-h\nu/kT)\}$ takes into account the effect of the induced emission; $I_{\nu p}$ is the intensity of the black body radiation as given by Planck's formula:

$$I_{\nu p} = \frac{2 h\nu^3}{c^2} \frac{1}{\exp(h\nu/kT) - 1} \quad (22)$$

Application of the law of Kirchhoff results in the following expressions for the continuum emission coefficient ϵ_{ν} :

$$\epsilon_{\nu} = \frac{32\pi^2}{3\sqrt{3}} \frac{e^6}{(4\pi\epsilon_0)^3} \frac{\gamma}{U_A} \frac{Z^{*2} kT n_A}{h^3 c^3} \exp(-I_A/kT) \quad (23)$$

$$\nu \leq \nu_g$$

*) This equation is frequently referred to as the Kramers-Unsöld formula.

$$\epsilon_{\nu} = \frac{32\pi^2}{3\sqrt{3}} \frac{e^6}{(4\pi\epsilon_0)^3} \frac{\gamma}{U_A} \frac{Z^{*2} kT n_A}{h^3 c^3} [\exp \{ (h(\nu_g - \nu) - I_A) / kT \}]$$

(24)

$$\nu > \nu_g$$

As can be seen from equation (23) the continuum emission coefficient is independent of the frequency for $\nu \leq \nu_g$. For $\nu > \nu_g$, ϵ_{ν} decreases proportionally to $\exp(-h\nu/kT)$.

Calculation of the bound-free absorption coefficient for photons whose energy is greater than the ionization energy of the complex atom ($h\nu > I_A$), making use of equation (18) gives rise to considerable deviations [9].

By employing the fact that these photons are mainly absorbed by atoms in the ground level, the following approximation formula can be derived for complex atoms [9]:

$$\alpha_{\nu} = \frac{32\pi^2}{3\sqrt{3}} \frac{e^6}{(4\pi\epsilon_0)^3} \frac{Z^{*2} n_A}{h^4 c \nu^3} \cdot I_A$$

(25)

$$h\nu > I_A$$

The value of Z^{*2} , according to Unsöld [10] and Vitense [12], is of the order of 4 to 7 for all levels which corresponds to the ground state of the atoms.

With the help of Kirchhoff's law, we find for the emission coefficient:

$$\epsilon_{\nu} = \frac{64\pi^2}{3\sqrt{3}} \frac{e^6}{(4\pi\epsilon_0)^3} \frac{Z^{*2}}{h^3 c^3} n_A \cdot I_A \cdot \exp(-h\nu/kT)$$

(26)

$$h\nu > I_A$$

It should be noted that the ionization energy I is decreased by an amount ΔI , as a result of electric micro-fields in the plasma generated by charge carriers. This correction must be introduced when calculating the coefficients α_{ν} and ϵ_{ν} .

The lowering of the ionization energy ΔI_z can be calculated by means of the Debye-Hückel approximation [1]:

$$\Delta I_z = 2 (Z + 1) \frac{e^3}{(4\pi\epsilon_0)^{3/2}} \left(\frac{\pi}{kT} \right)^{1/2} \cdot (n_e + \sum_i Z_i^2 n_i)^{1/2}$$

(27)

where:

- $k =$ Boltzmann's constant ($1.38 \cdot 10^{-23} \text{ J } ^\circ\text{K}^{-1}$)
 $\epsilon_0 =$ the vacuum permittivity ($\frac{100}{36\pi} \cdot 10^{-11} \text{ F m}^{-1}$)
 $n_e =$ the density of the electrons [m^{-3}]
 $n_i =$ the density of the particles i with electric charge $Z_i e$
 ($Z_i = 0$ for neutrals; $Z_i = 1$ for single ionized particles; etc.)

11-3. Line absorption and emission coefficients.

The dependence, as function of the frequency, of the absorption coefficient α'_ν of a spectral line is given by the following relationship, derived from the classical theory [13]:

$$\alpha'_\nu = \frac{\pi e^2}{(4\pi\epsilon_0)m_e c} n_j f_{jm} Q(\nu) (1 - \exp(-h\nu/kT)) \quad (28)$$

where n_j is the population density per unit volume of the energy level j ; f_{jm} is the oscillator strength for the transition of the lower level j to the higher level m and $Q(\nu)$ is the normalized line shape function ($\int Q(\nu) d\nu = 1$).

The population n_j of the energy level j is given, in the case of L.T.E., by:

$$n_j = n \frac{g_j}{U} \exp(-I_j/kT) \quad (29)$$

where n is the total particle density of the atoms or ions per unit volume; U is the partition function of the atoms or ions; g_j and I_j are the statistical weight and excitation energy of level j respectively. Application of Kirchhoff's law (equation (21) to equation (28) gives for the emission coefficient ϵ_ν :

$$\epsilon_\nu = \frac{2h\nu^3}{c^2} \frac{\pi e^2}{(4\pi\epsilon_0)m_e c} n_j f_{jm} Q(\nu) \exp(-h\nu/kT) \quad (30)$$

The line shapes of spectral lines are almost never determined by natural broadening only.

Besides natural broadening, Doppler broadening is always present and dominates the line shapes near the line centre at high temperatures or low densities.

However, in a high pressure discharge (pressure some atmospheres), the two above-mentioned universal line broadening mechanisms are often negligible, because the line shapes are strongly influenced by the interaction of the radiating atoms or ions with surrounding particles. This broadening mechanism is referred to as pressure broadening. Interaction with the radiating atoms or ions can be achieved by either neutral or charged particles. The effect of charged particles, however, is so much greater than that of neutral particles that the interaction of the latter can be neglected as soon as there is any appreciable ionization [14]. (For nitrogen at a pressure of a few atmospheres, this occurs when the temperature rises above 10^4 °K).

Hence there are two main broadening agents, ions and electrons. Because electric fields are involved, this type of broadening is called Stark broadening. A fundamental study of pressure broadening has been made by Baranger [14]. Based on this study Griem [15] calculated the Stark broadening of several elements and tabulated numerical results [16].

The shape of a line broadened by the Stark effect can be described, to a first approximation by a Lorentz function [17], which is given in normalized form by [13]:

$$L(\nu) = \frac{1}{\pi} \frac{1}{\beta_s} \frac{1}{1 + \left[\frac{\nu - \nu_{mj}}{\beta_s} \right]^2} \quad (31)$$

where ν_{mj} is the central line frequency and β_s is the half-half width for Stark broadening.

Figure 3 shows a Lorentz function, normalized on unity, as a function of the normalized frequency deviation $(\nu - \nu_{mj})/\beta_s$. The earlier mentioned Doppler broadening results in a Gaussian line shape, which is given in normalized form by [13]:

$$G(\nu) = \frac{1}{\sqrt{\pi}} \cdot \frac{1}{\beta_D} \exp \left[- \left[\frac{\nu - \nu_{mj}}{\beta_D} \right]^2 \right] \quad (32)$$

The half-half width of this function is given by [18]:

$$\beta_D \sqrt{\ln 2} = \frac{v_{mj}}{c} \sqrt{\frac{2kT}{M} \ln 2} = 1.48 \cdot 10^{-20} v_{mj} \sqrt{T/M} \quad (33)$$

where M is the mass of the emitting atoms.

When the half-half width due to the Stark effect (at high densities the natural broadening can be entirely neglected) is not appreciably greater than the half-half width due to the Doppler effect, the resultant line profile is obtained by folding the two line shapes $L_S(\nu)$ and $G_D(\nu)$, that is [19]:

$$V(\nu) = \int_0^{\infty} G_D(\nu') L_S(\nu - \nu') d\nu' \quad (34)$$

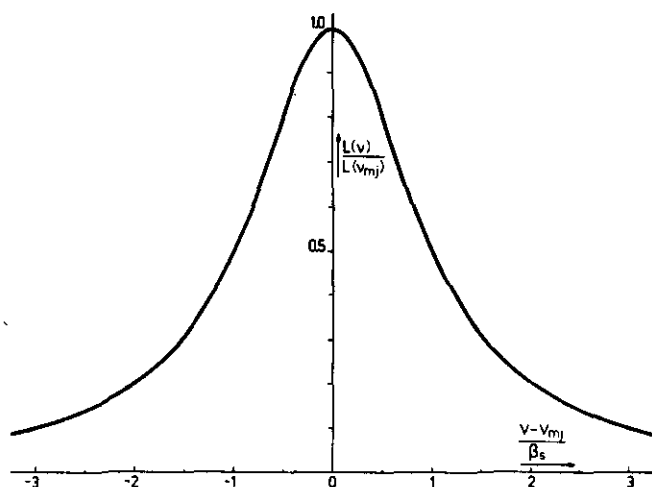


Fig. 3. Lorentz function.

This leads to Voigt profiles, which are available in both tabular and graphic form for a large number of conditions [20, 21, 22].

Figure 4 shows a number of normalized Voigt profiles as functions of the normalized frequency deviation k , with the ratio $\beta_S/\beta_D = \alpha$ as a parameter. The frequency deviation k is defined by: $k = (\nu - \nu_{mj})/w$, where w is the effective half-half width of the Voigt profile.

For $\alpha > 0.4$ a first approximation for w is given by [21]:

$$w \approx \sqrt{\beta_D^2 + \beta_S^2} \quad (35)$$

It is apparent from figure 4 that the Voigt functions for large values of k , i.e. in the "wings", behave as a Lorentz function. This is a result

of the fact that the Gauss function at large values of k approaches zero more rapidly than the Lorentz function.

The influence of the Gauss (Doppler) kernel on the Voigt functions becomes less as α increases.

For $\alpha > 1$, it appears that the Voigt profile, apart from a relatively small kernel, approximates well to the Lorentz profile.

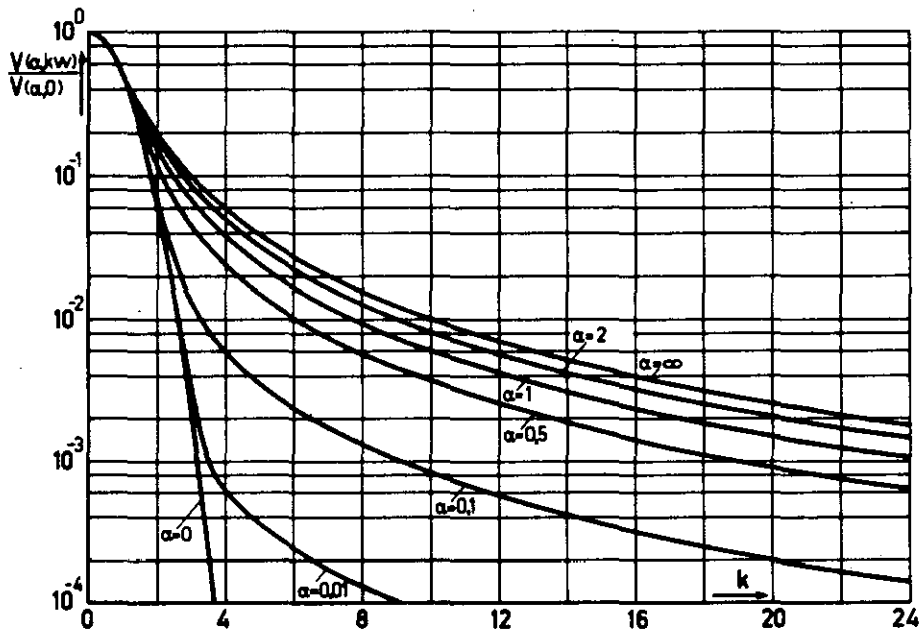


Fig. 4. Values of the function $V(\alpha, kw)/V(\alpha, 0)$ for some values of α .

III... Absorption and emission coefficients for the NI continuum and NI, NII lines.

III-1. The NI continuum.

Figure 5 reproduces part of the term diagram NI which has been taken from [23].

It can be seen from figure 5, that the 4P level in the $1s^2 2s^2 2p^2 3s$ system forms the lower limit of the group of strongly-excited levels, lying close together.

The lowering of the ionization energy ΔI , calculated by means of equation (27), is about 0.4 eV at a pressure of 3 atm.abs. and 0.5 eV at a pressure of 5 atm.abs.

The effective nuclear charge Z^* for the frequency interval $\nu \leq \nu_g$ ($9.38 \cdot 10^{14} \text{ sec}^{-1}$) has been calculated from the 2P and 4P levels of the $1s^2 2s^2 2p^2 ns$ system, from the $^2S^0$, $^2D^0$, $^4P^0$ and $^4D^0$ levels of the $1s^2 2s^2 2p^2 np$ system ($n > 2$) and the 2P , 2D , 2F , 4P , 4D and 4F levels of the $1s^2 2s^2 2p^2 nd$ system, employing equation (16) and is found to be about 1.4.

The effective nuclear charge Z^* for the frequency interval $\nu_g \leq \nu \leq \nu_{gh}$ has been calculated from the $3s^4P$ and from the $^2P^0$, $^2D^0$ and $^4S^0$ levels of the $1s^2 2s^2 2p^2 2p$ system, the resulting value being about 1.7.

If the quantities calculated above are inserted in equations (19) and (20), the following expressions for the absorption coefficient α_ν of the NI continuum are obtained:

$$\alpha_\nu = \frac{16\pi^2}{3\sqrt{3}} \frac{e^6}{(4\pi\epsilon_0)^3} \frac{(1.4)^2 kT n_N}{h^4 c \nu^3} \exp[-(I_N - \Delta I)/kT] \exp(h\nu/kT) \quad (36)$$

$$\nu \leq \nu_g$$

$$\alpha_\nu = \frac{16\pi^2}{3\sqrt{3}} \frac{e^6}{(4\pi\epsilon_0)^3} \frac{(1.7)^2 kT n_N}{h^4 c \nu^3} \exp[-(I_N - \Delta I)/kT] \exp(h\nu_g/kT) \quad (37)$$

$$\nu > \nu_g$$

In these equations I_N is the ionization energy of the nitrogen atom, (14.53 eV).

The corresponding expressions for α'_ν can be obtained by multiplying (36) and (37) with the term: $[1 - \exp(-h\nu/kT)]$.

It can be shown [26] that at pressures of several atmospheres, the mean free path of the photons: $\bar{x}_\nu = 1/\alpha'_\nu$ exceeds $5 \cdot 10^{-2} \text{ m}$ for that part of the spectrum where the frequency ν is smaller than ν_{gh} (principal series limit).

When a high-pressure discharge has a diameter d of a few millimeters, this means that for the NI continuum ($\nu \leq \nu_{gh}$) practically no reabsorption occurs: in other words, the discharge is optically thin for the NI continuum ($\nu \leq \nu_{gh}$).

The balance between the emitted and absorbed radiative energy per unit volume, time and frequency, u_ν is then given by:

$$u_\nu = e_\nu - a_\nu \approx e_\nu = 4\pi\epsilon_\nu \quad (38)$$

Substitution of the expressions for ϵ_ν found in equations (23) and (24) with the corresponding values for γ/U_N , Z^* and ΔI in equation (38) and integration over the corresponding frequency interval, gives the emission per unit time and volume of radiative energy e which leaves the discharge

($e \equiv u$).

The results of these calculations, as a function of temperature with pressure as a parameter, are reproduced in figure 6.

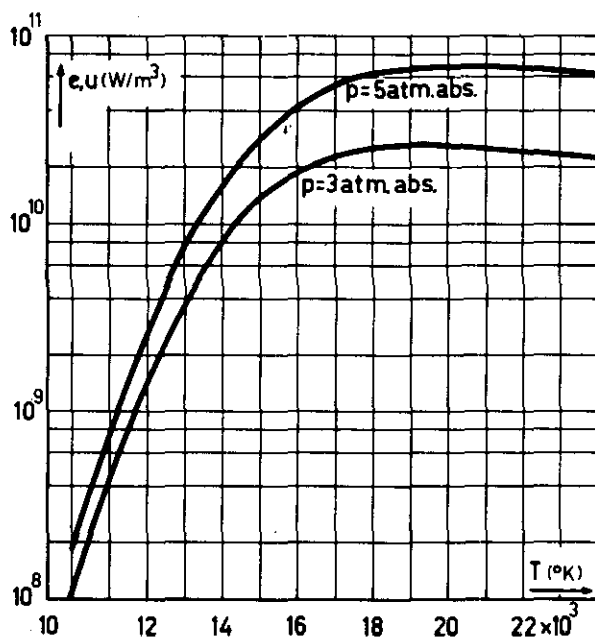


Fig. 6. Radiative energy per unit volume and time of the "optically thin" NI continuum ($\nu \leq \nu_{gh}$) as a function of the temperature with pressure as a parameter.

The bound-free absorption coefficient $\alpha_{\nu_{bf}}$ for high-energy photons ($h\nu > I_N - \Delta I$) is given, to a first approximation, by equation (25). Calculation of the effective charge Z^* , by means of equation (16) for the ground level of the nitrogen atom, gives a value of about 2. Substitution of the numerical values of the constants, e , ϵ_0 , h , c and Z^* in equation (25) results in the following expression for $\alpha_{\nu_{bf}}$:

$$\alpha_{\nu_{bf}} = 1.26 \cdot 10^{43} \frac{(2)^2 n_N}{\nu^3} (I_N - \Delta I) \quad (39)$$

$$\nu > \nu_{gh}$$

Multiplication of equation (39) by the term $(1 - \exp\{-h\nu/kT\})$, which takes into account the effect of the induced emission, gives the expression for $\alpha'_{\nu_{bf}}$.

Calculation of α'_{ν} according to (39) as a function of frequency at pressures of several atmospheres shows values for the mean free path of the photons $\bar{\lambda}'_{\nu} = 1/\alpha'_{\nu}$ of the order of 10^{-3} m [26]. Which means that the mean free path^{bf} of the photons $\bar{\lambda}'_{\nu}$ is of the same order as or much smaller than the diameter d , (d is several millimeters), of the discharge. For this part of the NI continuum ($\nu > \nu_{gh}$) re-absorption of emitted radiation will take place.

This implies that the absorbed radiative energy per unit volume, time and frequency a_{ν} is not equal to zero and therefore $u_{\nu} \neq e_{\nu}$.

III-2. The NI and NII lines.

It is worthwhile to divide the NI and NII lines, which have been taken from [24], into two groups:

- a) one group for which the central wave length $\lambda_{mj} < 2000 \text{ \AA}$ and
- b) one group for which $\lambda_{mj} > 2000 \text{ \AA}$.

For the lines in group b) we find that at a pressure of several atmospheres the half-half widths due to the Doppler effect, as calculated from equation (33) in a temperature range from about 10^4 to 2×10^4 °K, are small with respect to the Stark effect as calculated by Griem [16], ($\beta_S/\beta_D \geq 10$). In other words, for this group of lines the Stark effect is by far the most important broadening mechanism with the result that the line shapes can be described by a Lorentz function as given by equation (31).

Calculation of the absorption coefficients for the central line frequencies by means of equation (28), the data on NI and NII lines from the tables of Wiese et al. [24], the half-half widths from Griem's tables [16], produces values of the order of $\leq 1 \text{ m}^{-1}$. In other words, in a high pressure discharge (pressure a few atmospheres) with a diameter of several millimeters, no absorption will occur for this group of lines ($\lambda > 2000 \text{ \AA}$). The radiative energy per unit volume and time emitted by an $m \rightarrow j$ transition which leaves the discharge is then independent of the line shape and is given by:

$$e_{mj} = u_{mj} = h\nu_{mj} A_{mj} n_m \quad (40)$$

where u_{mj} is the balance between the emitted and absorbed radiative energy per unit volume and time; n_m is the population of the upper level m ; A_{mj} is the transition probability of the transition from the upper level m to the lower level j ; ν_{mj} is the central line frequency.

The total radiative energy per unit-volume and -time emitted by the NI and NII lines in group b) is obtained by employing equation (40) to calculate the term e_{mj} for each line and subsequently summing them over all the lines in the group.

The results of these calculations are shown in figure 7 as a function of temperature with pressure as parameter. The values, required for these calculations, for the transition probabilities A_{mj} ; the central line frequencies ν_{mj} ; statistical weights g_m ; excitation energies I_m , have been taken from the tables of Wiese et al. [24]; the particle densities n_N and n_{N+} and the partition functions U_N and U_{N+} have been taken from the tables of Pflanz et al. [25].

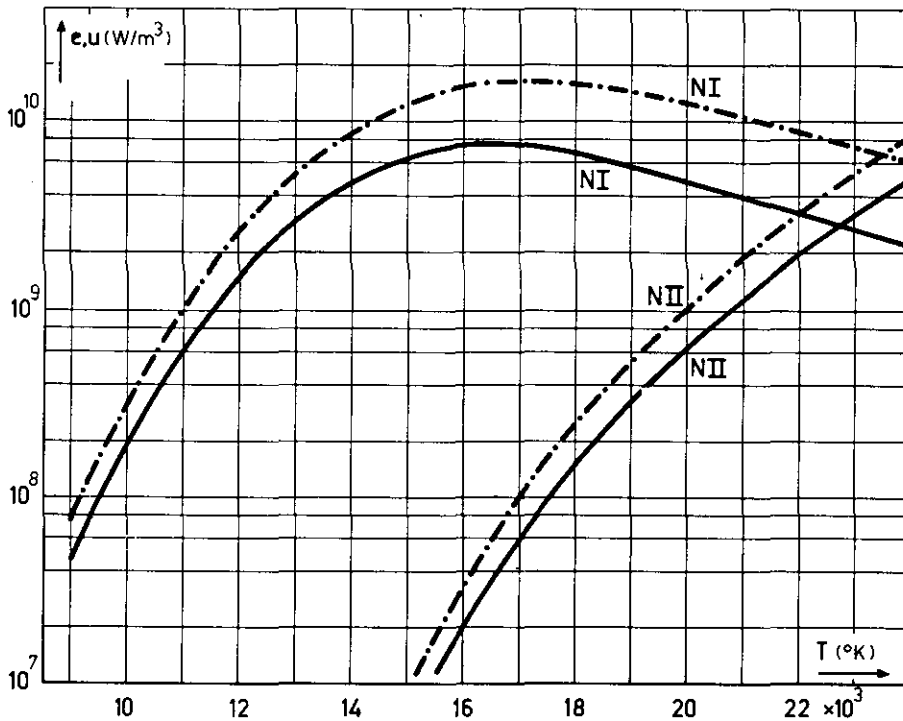


Fig. 7. Radiative energy per unit volume and per unit time of the NI and NII lines ($\lambda_{mj} > 2000 \text{ \AA}$) as a function of temperature.
 Solid lines: $p = 3 \text{ atm. abs.}$; Dashed lines: $p = 5 \text{ atm. abs.}$

Calculation of the Doppler half-half widths for the lines in group a) ($\lambda_{mj} < 2000 \text{ \AA}$), at pressures at several atmospheres and in a temperature range from about 10^4 to $2 \times 10^4 \text{ }^\circ\text{K}$, gives values which are of the same order as the Stark half-half widths calculated by Griem [16]. ($\beta_S/\beta_D \approx 1$). This means that the line form is given by a Voigt function as indicated in figure 4. Calculation of the absorption coefficients for the central line frequencies α'_v according to equation (28); values of the Voigt functions for $k = 0$ from Posener's tables [21] and data on the NI and NII lines from the tables of Wiese et al. [24], gives values of the order of $\geq 10^5 \text{ m}^{-1}$. In other words, a high pressure discharge with a diameter of several millimeters is optically thick for this group of lines for relatively large values of the frequency deviation k (see figure 4).

Contribution by a line in this group to the radiative balance u_{mj} can only take place by means of the "wings" of this line.

From figure 4 appears that the Voigt functions for $\alpha = \beta_S/\beta_D \approx 1$ and large values of k , i.e. in the "wings", behave practically as a Lorentz function. In other words, in calculating the radiative energy transfer by the NI and NII lines ($\lambda_{mj} < 2000 \text{ \AA}$) in a high pressure discharge, the required line shape is given to a good approximation by a Lorentz function with a half-half width w given by equation (35).

IV. Description of the computer programmes for the calculation of the radiative balance in a cylinder symmetric discharge.

IV-1. Introduction.

The radiative balance U , which is part of the total energy balance of a discharge, is the difference between the emission e and the absorption a of radiative energy per unit time and volume: $u = e - a$. All three terms contain contributions from the whole spectrum.

As already stated in the foregoing chapters, integration over the whole volume of the discharge is necessary for the calculation of the absorbed energy per unit time, frequency and volume a_v at a given point in the discharge, for that part of the spectrum for which the discharge is "optically thick"; i.e. the mean free path of the photons $\bar{\lambda}_v$ is smaller than the diameter of the discharge. This implies that, for this part of

the spectrum, the spectral emission and absorption, coefficients ϵ_{ν} and α_{ν} must be known for every point in the discharge. Since ϵ_{ν} and α_{ν} are known functions of the temperature (Chapter II and III) it is sufficient if the temperature distribution in the discharge is known.

For the calculation of the contribution to the radiative balance for that part of the spectrum for which the discharge is optically thick a number of computer programmes have been developed.

The complete text of these programmes is given in the Appendices II, III and IV. The programmes have been written in "ALGOL 60". These computer programmes are described in the following sections.

IV-2. The exponential integral B(g).

As appears from (10), the calculation of $a_{\nu}(r)$ requires a four dimensional integration over r , r_0 , ϕ and θ . The calculation of $a(r)$ requires moreover an integration over the frequency ν . In order to restrict the number of integrations to be performed, the exponential integral:

$$B(g) = \int_0^{\pi/2} \exp(-g/\cos\theta) d\theta, \text{ as a function of } g \text{ has been calculated}$$

only one time. The calculation of the function $B(g)$ has been performed for $0 \leq g \leq 15$, with the steplengths of g being 0.01. For values of $g > 15$, $B(g)$ has been taken equal to zero, this can be employed because in that case $B(g)$ is smaller than $10^{-7} B(0)$.

The integration of the exponential function causes some problems owing to the singular point in the exponent of the integrand for $\theta = \pi/2$. Therefore, it is essential to choose an upper limit for the integration and to make an estimation of the error consequently made.

θ_1 being the upper limit of the integral for which: $0 < \theta_1 < \pi/2$ then follows:

$$\int_0^{\pi/2} \exp(-g/\cos\theta) d\theta = \int_0^{\theta_1} \exp(-g/\cos\theta) d\theta + \int_{\theta_1}^{\pi/2} \exp(-g/\cos\theta) d\theta \quad (41)$$

The upper limit θ_1 must be chosen such that $\int_{\theta_1}^{\pi/2} \exp(-g/\cos\theta) d\theta \leq \Sigma$

in which Σ is the permissible error in the estimation. By taking θ_1 larger or equal to:

$$\theta_1 \geq \arccos \left[\frac{g}{14.85+g - \ln \left(\arccos \frac{g}{g+2.3} \right)} \right] \quad (42)$$

the error in the estimation of the exponential integral $B(g)$ is smaller or equal:

$$\Sigma \leq \frac{10^{-6}}{1.8} \arccos \left(\frac{g}{g-1n0.1} \right) \quad (43)$$

In table I the calculated values for θ_1 and Σ , as a function of g , are shown.

TABLE I.

g	θ_1 [radians]	Σ
0.1	1.5639	7.6869 10^{-7}
0.5	1.5375	4.6886 10^{-7}
1	1.5067	2.5816 10^{-7}
2	1.4512	8.1753 10^{-8}
4	1.3584	8.9871 10^{-9}
6	1.2827	1.0509 10^{-9}
8	1.2193	1.2704 10^{-10}
10	1.1649	1.5683 10^{-11}
12	1.1176	1.9639 10^{-12}
15	1.0960	8.8678 10^{-14}

The text of the programme for calculating the exponential integral $B(g)$ with θ_1 as upper limit, in accordance with (42), is given in Appendix I. The results of the calculations are shown in fig. 8. The values for $B(g)$, calculated with the aid of procedure $B(g)$ (see Appendix I) as a function of g , are supplied by the computer on a punched tape.

Each time a programme is run for the calculation of the radiative balance, this tape has to be read in.

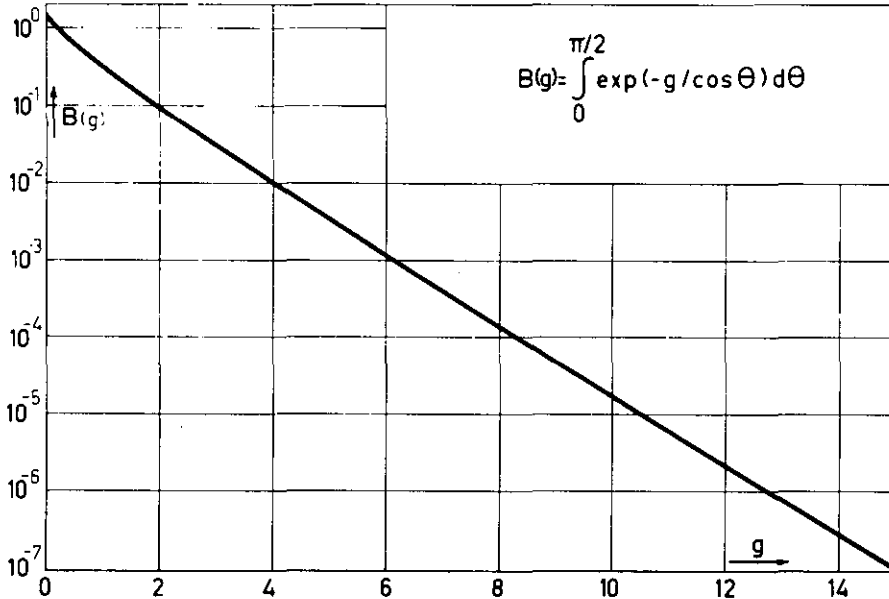


Fig. 8. The exponential integral $B(g)$ as a function of g .

In these programmes (see Appendices II, III and IV) the $B(g)$ table is processed as follows:

Each time when, at a defined value of g , the computer asks for the relevant value for $B(g)$, an appeal is made to the procedure $B(g)$ (see Appendices II, III and IV).

In this procedure it is defined whether the value for g , indicated by the computer, is in the range for which the $B(g)$ table applies. If not, then the largest respectively the smallest value of B is supplied if g is too small or too large. Now, the table can be considered as being the interval on which B must lie. By dividing this interval into approximately equal parts and, next determination in which half g lies, the range containing g can successively be reduced until the interval in which g lies has been reduced to two successive values in the table:

$$g[i] \leq g \leq g[i + 1] \quad (44)$$

With the aid of linear interpolation the relevant value of $B(g)$ can be determined:

$$B(g) = \frac{B[i + 1] - B[i]}{g[i + 1] - g[i]} \cdot (g - g[i]) + B[i] \quad (45)$$

A flow diagram of the procedure B(g) is given in figure 9.

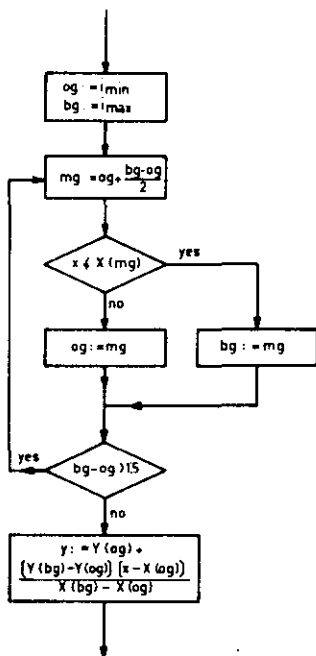


Fig. 9. Flow diagram of the method of linear interpolation.

IV-3. Calculation of the absorption and emission coefficient.

As is shown in chapter II the spectral emission and absorption coefficients are known functions of the temperature. The calculation of the coefficients as a function of position in a discharge requires the knowledge of the temperature distribution $T(r)$ in that discharge. This temperature distribution must be added to the input data to the computer.

Calculation of the temperature at a given value for the radius r takes place by linear interpolation in this table of radius and relevant temperature values. This interpolation is performed in the same way as that for $B(g)$ (see section IV-2).

The dependence as a function of the frequency of the absorption coefficient α'_ν of a spectral line, in a point r_Q in a high-pressure, high-temperature discharge is given to a first approximation by (see chapter II and III):

$$\alpha'_\nu(r_Q) = \alpha'_\nu(T(r_Q)) = \frac{\pi e^2}{(4\pi\epsilon_0)m_e c} \cdot n(T(r_Q)) \cdot \frac{g_j \exp[-I_j/kT(r_Q)]}{U} f_{jm}$$

$$\frac{1}{\pi} \frac{1}{w(T(r_Q))} \frac{1}{1 + \left[\frac{Aw(T(r_A))}{w(T(r_Q))} \right]^2} \cdot [1 - \exp(-h\nu/kT(r_Q))] \quad (46)$$

where:

- n the density of the atoms or ions
- U the partition function of the atoms or ions
- A integer
- w the effective half-half width of the Voigt profile.

An expression for w has already been given by (35).

The half-half width due to the Stark effect, β_S is given to a first approximation by [27]:

$$\beta_S(r_Q) = \beta_S(T(r_Q)) = \frac{c}{\lambda_{mj}} w_{tab} n_e(T(r_Q)) 10^{-22} [\text{sec}^{-1}] \quad (47)$$

where:

- n_e density of the electrons
- c velocity of light in vacuum
- w_{tab} reduced half-half width due to the Stark effect [m]

The values of w_{tab} for the relevant spectral lines are taken from the tables in [16]. An expression for the half-half width due to the Doppler effect β_D has already been given by (33).

As can be seen from (46) the frequency deviation $\Delta\nu$ is given by:

$$\Delta\nu = \nu_{mj} - \nu = A w (T(r_A)) \quad (48)$$

The frequency deviation is thus related to the half-half width $w(T(r_A))$ in point r_A ; i.e. that point in the discharge in which we want to calculate the radiative balance.

The relevant value for the spectral emission coefficient $\epsilon_\nu(r_Q)$ is found by multiplying (46) with the intensity $I_{\nu p}$ of a black body radiator, this gives:

$$\epsilon_\nu(r_Q) = \epsilon_\nu(T(r_Q)) = \alpha'_\nu(T(r_Q)) \cdot \frac{2h\nu^3}{c^2} \frac{1}{\exp\{h\nu/kT(r_Q)\} - 1} \quad (49)$$

The particle densities of the atoms or ions and electrons n , n_e and the partition functions for the atoms or ions U found in the expressions for the spectral absorption and emission coefficient must - as a function of the temperature- be added to the input data to the computer.

Using the procedure ORTHOPOL these series of values for n , n_e and U are approximated by systems of orthogonal polynomials. With the procedure YAPPROX the values of n , n_e and U can be calculated if the temperature is given. The procedures ORTHOPOL and YAPPROX are standard procedures of the computer centre of the Eindhoven University of Technology.

For more information about these procedures reference is made to [28]. The calculation of ϵ_ν and α_ν^l is performed in the procedures written for that purpose. (Appendix II and IV: procedures EPSILONU (R) and ALPHANU (R); Appendix III: procedure epsilon (r) and procedure alpha (r)).

It should be noted that in these procedures the effective half-half width w is represented by β_1 ; β_S by β_2 and β_D by β_3 . The frequency dependence of the spectral absorption and emission coefficients is calculated in the procedure EEN(A).

IV-4. Calculation of the contribution of a spectral line to the radiative balance in the axis of the discharge.

From (13) appears that the calculation of the absorbed radiative energy per unit volume, time and frequency in the axis of the discharge $a_\nu(o)$ requires a two dimensional integration. The calculation of g is performed using the trapezium rule. This is a simple integration method requiring little execution time. For the integration over r_Q a second-order Runge-Kutta method has been employed:

$$\int_{x_0}^{x_2} f(x) dx \approx \frac{h}{3} [f(x_0) + 4f(x_1) + f(x_2)] \quad (50)$$

where h is an equidistant step length.

This method is also known as the Simpson rule.

Worked out this gives:

$$\int_{x_0}^{x_{2n+2}} f(x) dx = \frac{h}{3} [f(x_0) + 4\sum_{k=0}^n f(x_{2k+1}) + 2\sum_{k=1}^n f(x_{2k}) + f(x_{2n+2})] \quad (51)$$

An improvement of the accuracy of the calculation process can be achieved by not taking the radius of the discharge R for the upper limit in the

integration over r_Q , but fifteen times the mean free path of the photons $\bar{\lambda}_\nu$, unless this exceeds R . In that case the radius of the discharge is taken for the upper limit.

For r_Q equals $15 \bar{\lambda}_\nu$, g is ($g = \int_0^{r_Q} \alpha'_\nu(r) dr$) of the order 10. From figure 8 then follows that $B(g)$ is of the order $10^{-5} B(0)$, in other words, the integration can be terminated. The above is carried out in the procedure INTEGRAND (a) (see Appendix II).

Figure 10 represents a flow diagram of this procedure.

After calculation of $\alpha'_\nu(0)$ and $\epsilon_\nu(0)$ there remains the calculation of $a(0)$ and $e(0)$ ($e = 4\pi \int \epsilon_\nu dv$) which requires an integration over the frequency ν . From (46) follows that α'_ν , as a function of the frequency deviation $\Delta\nu = A\omega$ behaves as $\frac{1}{1+A^2}$; therefore the integration can be carried out for $0 \leq A \leq 1000$, without essentially influencing the accuracy of the calculation:

$$a = \int_0^\infty a_\nu dv \approx \int_{\nu_{mj}-1000\omega}^{\nu_{mj}+1000\omega} a_\nu dv = 2\omega \int_0^{1000} a_\nu(A) dA \quad (52)$$

$$e = \int_0^\infty 4\pi \epsilon_\nu dv \approx 2\omega \int_0^{1000} 4\pi \epsilon_\nu(A) dA$$

The difference between e and a produces the contribution of the spectral line to the radiative balance.

The integration over the frequency is performed in the procedure TRAPEX (see Appendices II, III and IV).

This procedure is a standard procedure of the computer centre. For detailed information about this procedure referende is made to [29, 30].

Figure 11 represents, as illustration, $\epsilon_\nu(A)$, $a_\nu(A)$ and their difference $u_\nu(A)$ of a spectral line in the axis of the discharge.

The complete text of the programme for the calculation of the contribution of a spectral line to the radiative balance in the axis of a discharge is shown in Appendix II.

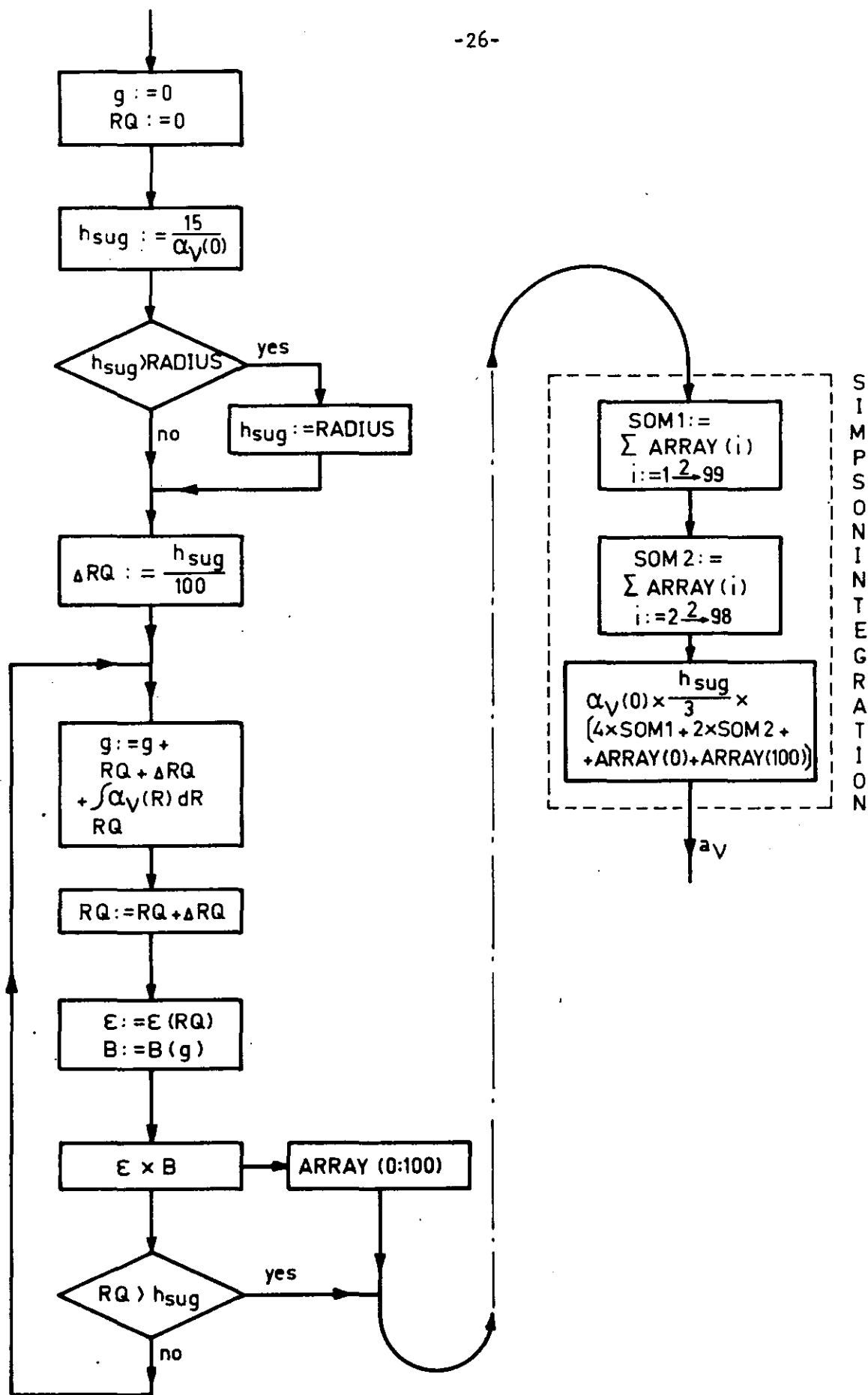


Fig. 10. Flow diagram of the procedure INTEGRAND (a).

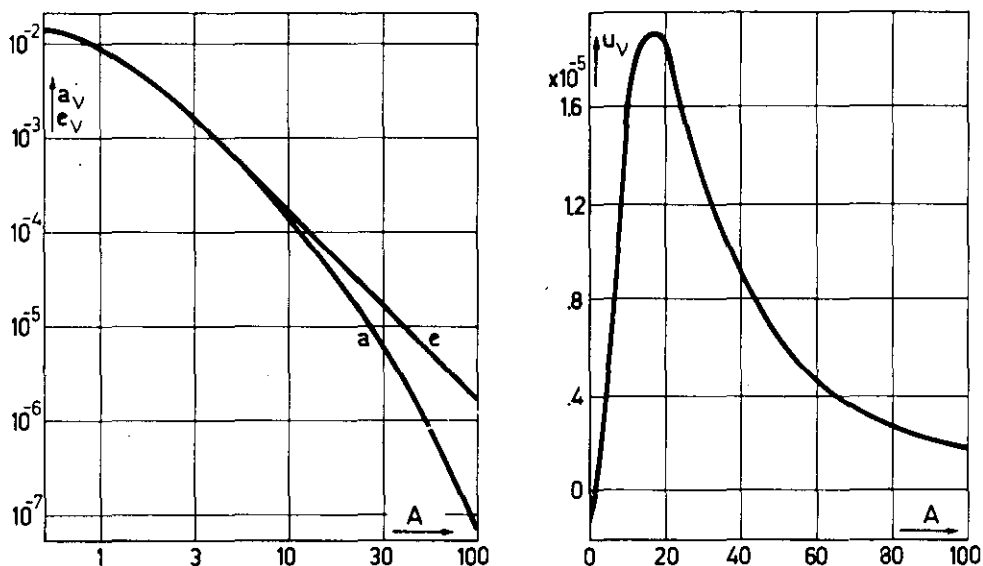


Fig. 11. Emission e_v , absorption a_v and their difference u_v as a function of the frequency deviation A .

IV-5. Calculation of the contribution of a spectral line to the radiative balance in points out of the axis of a discharge.

From the relation (10) for $a_v(r_A)$ appears that for $r_Q \approx r_A$ and $\phi \approx 0$ the integrand in (10) increases very rapidly ($\sqrt{r_A^2 + r_Q^2 - 2r_A r_Q \cos\phi} = s \rightarrow 0$). owing to which numerical integration with the here relatively large step is no longer possible. To prevent this singular point a constant has been added to the term s . This constant has the value $10^{-2} \bar{\lambda}_{v_{mj}}(r_A)$ with $\bar{\lambda}_{v_{mj}}$ the mean free path of the photons with frequency ν_{mj} (central line frequency). By applying this approximation the integration could be carried out properly.

It appeared that the accuracy of the calculation had not been influenced. The following method has been applied for the calculation of $a_v(r_A)$: To achieve a larger accuracy of the calculation process the integration limits for r_Q and ϕ have been established as follows:

<u>variable r_Q:</u>	upper limit	$r_Q = r_{\max} = r_A + 15 \bar{x}_v(r_A)$	(53)
		if $r_{\max} > R$, then $r_{\max} = R$	
	lower limit:	$r_Q = r_{\min} = r_A - 15 \bar{x}_v(r_A)$	
		if $r_{\min} \leq 0$, then $r_{\min} = 0$	
<u>variable ϕ:</u>	upper limit:	$\phi_{\max} = \arctan \frac{15 \bar{x}_v(r_A)}{\sqrt{r_A^2 - [15 \bar{x}_v(r_A)]^2}}$	
		if $15 \bar{x}_v(r_A) \geq r_A$, then $\phi_{\max} = \pi$	
	lower limit:	$\phi_{\min} = 0$	

The area within the integration limits is divided into four sub-areas (a, b, c and d) as shown in figure 12.

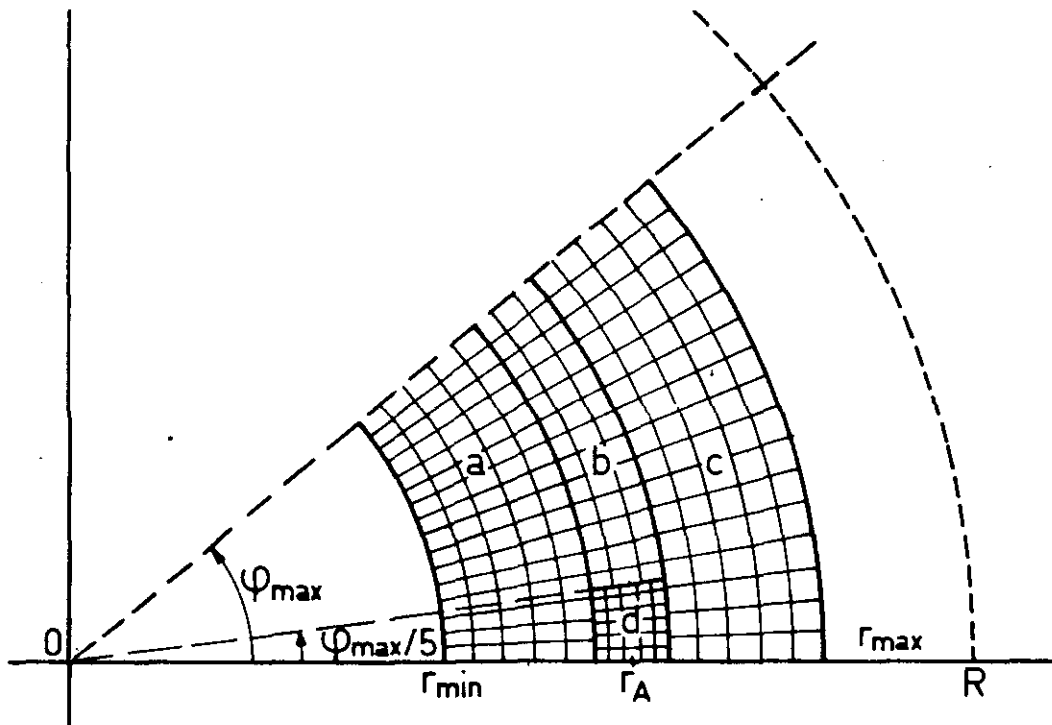


Fig. 12.

The limits of the variable r_Q in the sub-area d are given by:

upper limit:	$r_A + 1/5 (r_{\max} - r_A)$	(54)
lower limit	$r_A - 1/5 (r_{\max} - r_{\min})$	

Each of these four sub-areas is divided in the r and ϕ direction into surface elements. The number of surface elements in the sub-areas a, b and c is determined by staptal; that of sub-area d by staptal 1.

For staptal 1 choosing a value of the order of the value for staptal, achieves that the sub-area d is divided into much smaller surface elements than the sub-areas a, b and c resulting in a larger accuracy of the calculation process. For each surface element the value for g is determined from which with the aid of procedure B(g) the contribution of each element to the integrand of (10) is determined. Using procedure SIMPSON all these contributions are summed. In the calculation of g which is given by (12) the following approximation is applied (see figures 13 and 1):

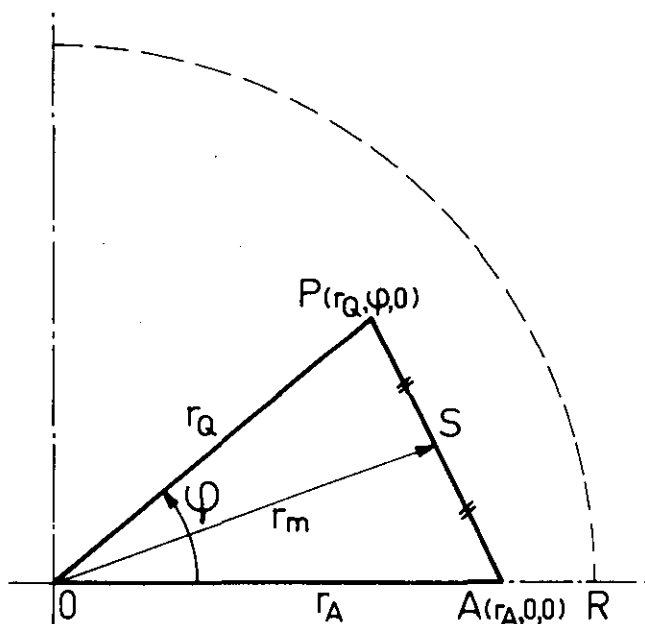


Fig. 13.

$$g = \int_P^A \alpha'_V(s) ds \approx \frac{s}{6} [\alpha'_V(r_A) + 4\alpha'_V(r_m) + \alpha'_V(r_Q)] \quad (55)$$

where r_m is given by:

$$r_m = \frac{1}{2} \sqrt{2r_A^2 + 2r_Q^2 - s^2} \quad (56)$$

The calculation of $\alpha'_V(r_Q)$ is carried out in the procedure anu(a) (See Appendix III).

The integration over the frequency is also performed using procedure TRAPEX. The complete text of the programme for the calculation of the contribution of a spectral line to the radiative balance in points out of the axis of the discharge is given in Appendix III.

IV-6. Calculation of the contribution of the bound-free continuum ($h\nu > I$) to the radiative balance in a cylindrically symmetric discharge.

Basically the calculation of the contribution of the bound free continuum ($h\nu > I$) to the radiative balance can be carried out in the same way as the calculations of the corresponding contributions of the spectrallines provided, the relevant expressions for the spectral absorption and emission coefficients, respectively indicated in the expressions (25) and (26), are introduced with regard to the integration over the frequency the existing programme, (see Apperidices II and III) have to be changed.

The frequency interval over which integration has to be performed has ν_{\min} as lower limit and ν_{\max} is given as upper limit.

The lower limit ν_{\min} is given by:

$$\nu_{\min} = \frac{I}{h} \quad (57)$$

For the upper limit ν_{\max} , ten times ν_{\min} has been choosen.

To prevent that the existing programmes have to be changed too drastically, an imaginary half-half width w_f has been introduced, which is given by:

$$w_f = \frac{\nu_{\max} - \nu_{\min}}{1000} \quad (58)$$

so that:

$$a = \int_0^{\infty} a_{\nu} d\nu \approx \int_{\nu_{\min}}^{\nu_{\max}} a_{\nu} d\nu = w_f \int_0^{1000} a_{\nu}(A) dA \quad (59)$$

The integration over the frequency is performed using the TRAPEX procedure.

It should be noted that this procedure (see Appendix IV) the imaginary half-half width is represented by BR0.

As an example the complete text of the programme for the calculation of the contribution to the radiative balance of the bound-free continuum in the axis of a discharge is represented in Appendix IV.

V. Radiative losses in discharges in a forced gas flow.

V-1. Temperature distributions.

In the figures 14, 15 and 16 the radial temperature distributions in discharges in a forced gas flow for a number of conditions (indicated in the figures) are shown. These temperature distributions, which are taken from [26], are determined by means of the relative side-on intensity distribution of a part of the NI free-free and free-bound continuum.

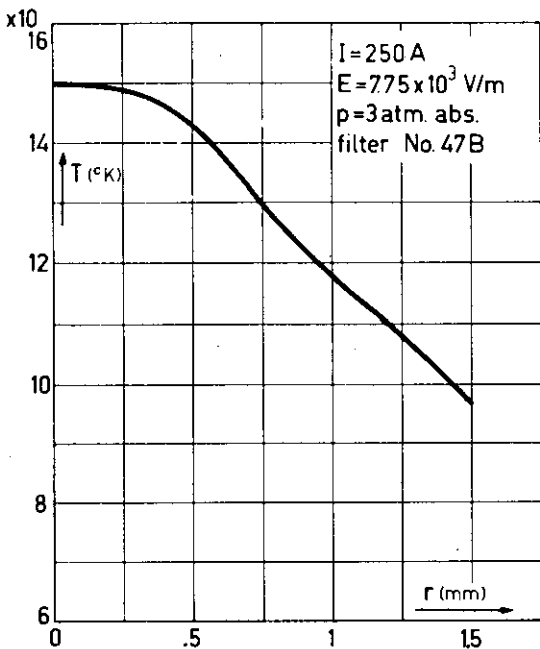


Fig. 14.

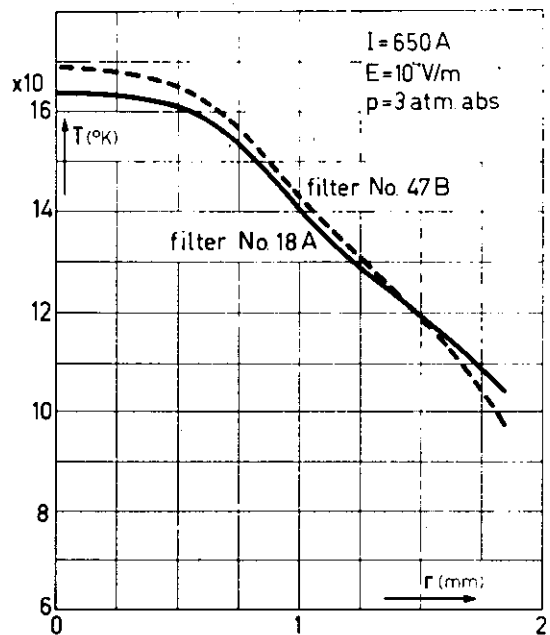


Fig. 15.

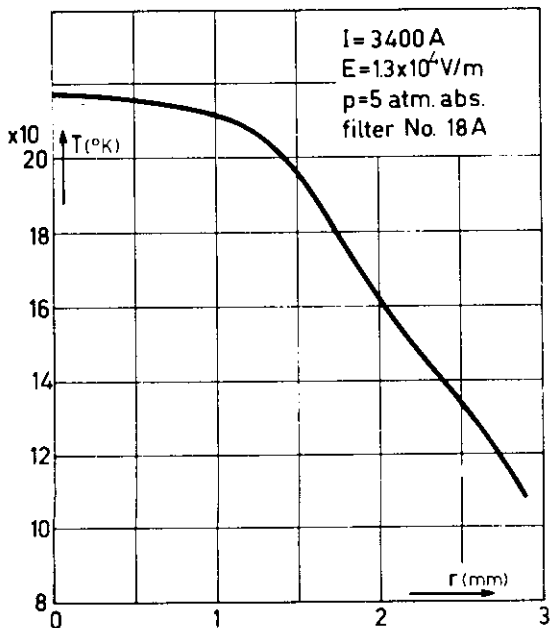


Fig. 16.

Temperature distributions as function of the radius, taken from [26].

In the next section, the radiative energy balance u , will be calculated as a function of the radius of the discharge, for the three temperature distributions indicated above.

V-2. The radiative balance.

The calculation of the contribution to the radiative energy balance by the NI and NII lines and the NI continuum for which the discharge is optically thick are performed by the computer programmes indicated in the appendix.

As already mentioned in chapter III are discharges at a pressure of some atmospheres and a diameter of a few millimeters. optically thick for those NI and NII lines for which the central wave length λ_{mj} is shorter than 2000 \AA and for that part of the NI continuum for which: $\nu > \nu_{gh}$ the principal series limit ($3.38 \cdot 10^{15} \text{ sec}^{-1}$).

The NI and NII lines under consideration have been taken from tables by Wiese et al. [24] and reproduced in table II. (For multiplets, only the strongest line is given).

The following procedure was adopted for the calculation of the contribution of the spectral lines:

First of all, for each line of a multiplet the separate contribution to the radiative energy balance was calculated for the centre of the discharge ($r = 0$). This point was chosen because, as a result of the symmetry, the integration over the angle ϕ in (10) can be carried out directly, which involves less work. Next we determined for each multiplet the factor M , by which the contribution of the strongest line (u_1) must be multiplied in order to obtain of the whole multiplet to the radiative energy balance.

The factor M is given by:

$$M = \frac{\sum_1^n u_k}{u_1} \quad (60)$$

where n is the number of lines in the multiplet and u_k the contribution of line k to the radiative energy balance.

This method can be employed because the lines of a multiplet lie very close together on the frequency / wave-length scale; it has been carried out, amongst others, in [31]. By using the factor M for the multiplets, the number of NI and NII spectral lines to be dealt with was reduced to that given in table II (reduction approx. factor 3).

TABLE II.

NI lines

Multiplet	λ [Å]	I_j [cm^{-1}]	I_m [cm^{-1}]	g_j	g_m	A_{mj} [10^8sec^{-1}]	f_{jm}
$2p^{34}S^0-3s^4P$	1199.55	0.0	83366	4	6	5.5	0.18
$2p^{32}D^0-3s^2P$	1492.62	19224	86221	6	4	5.3	0.12
$2p^{34}S^0-2p^4P$	1134.98	0.0	88110	4	6	2.2	0.064
$2p^{32}D^0-3s^1D$	1243.17	19224	99663	6	6	4.3	0.10
$2p^{32}P^0-3s^2P$	1742.73	28840	86221	4	4	1.8	0.082
$2p^{32}D^0-3d^2F$	1167.45	19224	104883	6	8	1.1	0.030
$2p^{32}P^0-3s^1D$	1411.94	28840	99663	6	10	0.52	0.026
$2p^{32}P^0-3d^2D$	1310.54	28840	105144	4	6	1.3	0.050
$2p^{32}P^0-3d^2P$	1319.72	28840	104615	4	4	1.1	0.029
$2p^{32}D^0-4s^2P$	1176.4	19224	104227	6	4	0.95	0.013
$2p^{32}D^0-3d^2D$	1163.88	19224	105144	6	6	0.43	0.0087
$2p^{32}D^0-5s^2P$	1100.7	19228	110082	10	6	0.33	0.0036
$2p^{32}P^0-4s^2P$	1326.63	28840	104227	4	4	0.15	0.0040
$2p^{32}D^0-3d^4F$	1169.69	19224	104718	6	8	0.030	0.00082
$2p^{32}P^0-3d^2F$	1316.29	28840	104811	4	6	0.025	0.00096
$2p^{32}P^0-5s^2P$	1231.7	28840	110029	2	2	0.022	0.0005

NIi lines

$2p^{23}P-2p^{33}D^0$	1085.70	131.3	92238	5	7	5.7	0.14
$2p^{23}P-2p^{33}P^0$	916.700	131.3	109218	5	5	13	0.17
$2p^{21}D-2p^{31}D^0$	775.957	15316	144189	5	5	49	0.45
$2p^{23}P-2p^{33}S^0$	645.167	131.3	155130	5	3	62	0.23
$2p^{21}D-2p^{31}P^0$	660.28	15316	166766	5	3	77	0.30
$2p^{21}D-3s^1P^0$	746.976	15316	149189	5	3	20	0.10
$2p^{23}P-3s^3P^0$	671.391	131.3	149077	5	5	9.9	0.067
$2p^{23}P-3d^3D^0$	533.726	131.3	187493	5	7	36	0.22
$2p^{21}D-3d^1F^0$	574.650	15316	189336	5	7	35	0.24
$2p^{21}S-2p^{31}P^0$	745.836	32687	166766	1	3	16	0.40
$2p^{23}P-3d^3P^0$	529.86	131.3	188858	5	5	15	0.062
$2p^{21}D-3d^1D^0$	582.15	15316	187092	5	5	13	0.064
$2p^{21}S-3d^1P^0$	635.180	32687	190121	1	3	18	0.32
$2p^{21}D-3d^1P^0$	572.07	15316	190121	5	3	0.97	0.0029

The results of the calculations of the separate contributions of the "optically thick" NI and NII lines and the NI continuum to the radiative energy balance, for the three temperature distributions with a central temperature of 15,000, 16,900 and 21,750 °K, are shown as a function of the radius in figures 17, 18 and 19 respectively.

The contributions of the part of the spectrum for which these discharges are optically thin, have already been given as a function of the temperature with pressure as parameter in figures 6 ("optically thin" NI continuum) and 7 ("optically thin" NI and NII lines).

Combining these with the given temperature distributions, we can derive the radial distributions of the "optically thin" contributions to the radiative energy balance. These results are also shown in figures 17, 18 and 19. The radial distributions of the total radiative energy balance (u_{total}), i.e. the sum of all the separate contributions, are given in figures 20, 21 and 22 respectively.

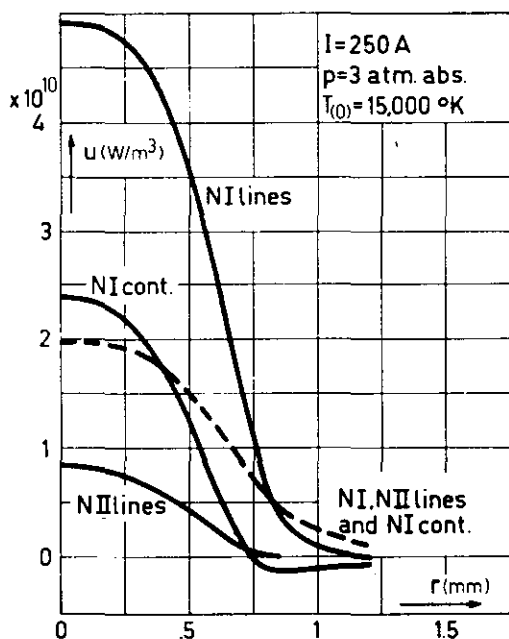


Fig. 17

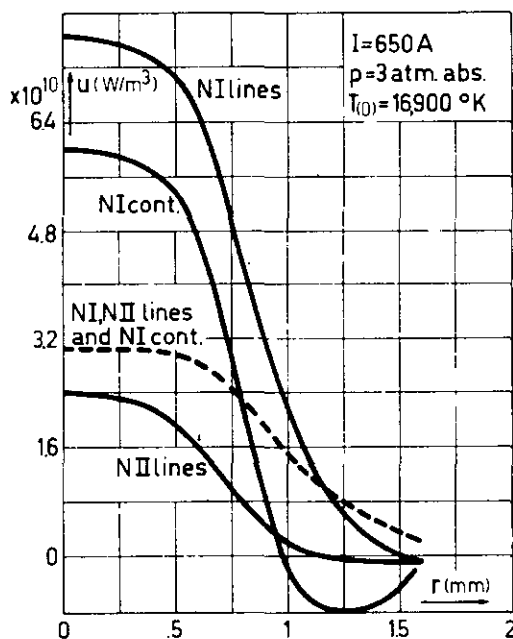


Fig. 18.

Also included in these figures is the radial distribution of one tenth of the electrical energy supplied per unit time and volume ($0.1 \sigma E^2$).

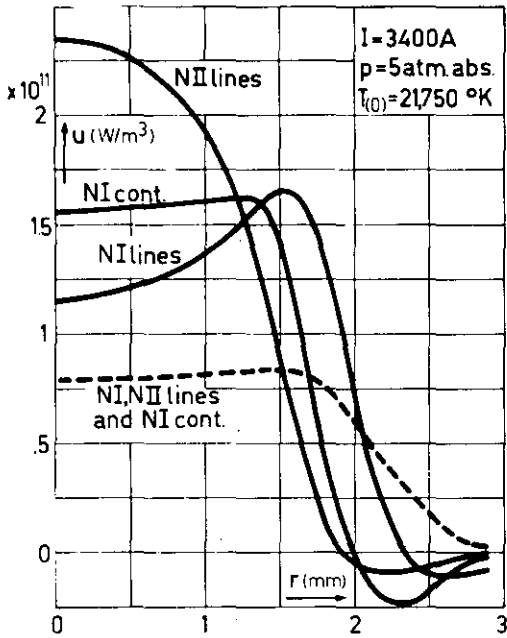


Fig. 19.
 Figures 17 to 19:
 Radial distribution of the contributions of the NI and NII lines and the NI continuum to the radiative energy balance.

— "optically thick"
 ---- "optically thin"

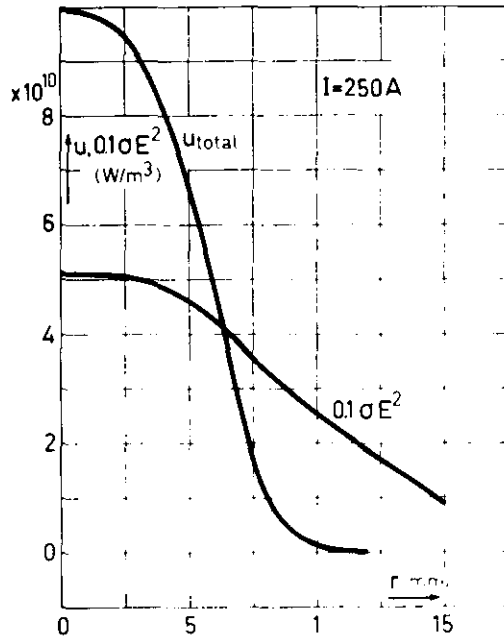


Fig. 20.
 Radial distribution of the radiative energy balance.

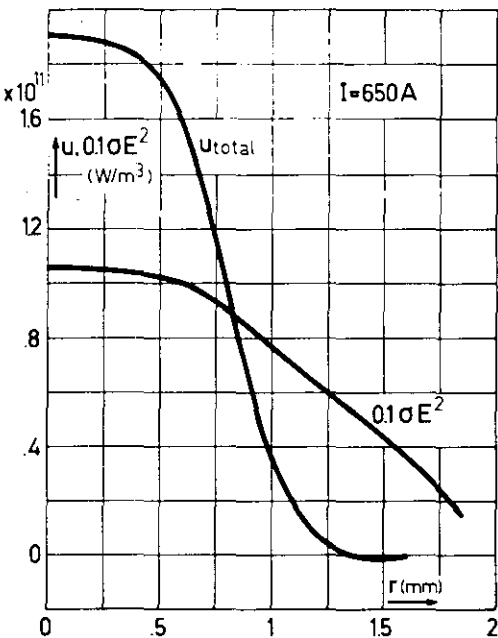


Fig. 21.
 Radial distribution of the radiative energy balance.

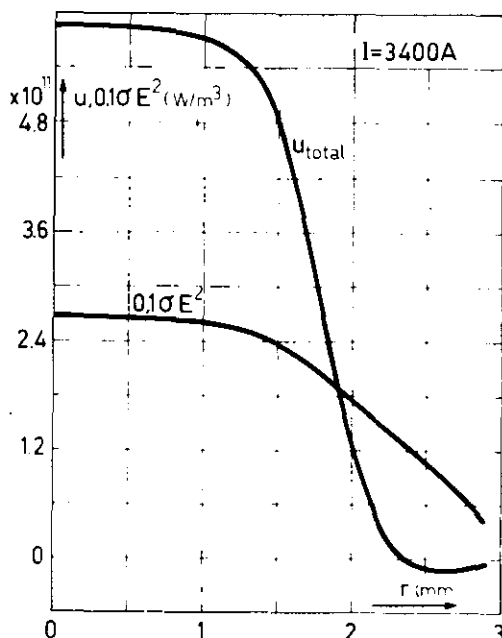


Fig. 22.

The electrical conductivity σ as a function of temperature and pressure as a parameter has been taken from [26].

From figures 20, 21 and 22 can be seen that the calculated energy dissipation by radiation (u_{total}) in the immediate neighbourhood of the centre is about 20 percent of the electrical energy supplied, but for greater values of the radius r ($r < R$) the importance of this energy dissipation decreases rapidly. At the boundary of the discharge ($r = R$) u_{total} is seen to become negative, indicating that at the edge of the discharge more radiative energy is absorbed than emitted, but this can be neglected with respect to the supplied electrical energy.

Calculations of the radial distributions of the radiative energy balance in "cascade arcs in nitrogen and argon" carried out by Uhlenbusch [32] and Hermann et al. [33] also produced negative values for u_{total} at the boundary of the discharge.

As a conclusion it can be stated that the radiation losses which occur in discharges at pressures of a few atmospheres and central temperatures of about 20,000 °K, when compared with the electrical energy supplied, are only of importance in the neighbourhood of the centre of the discharge.

Literature.

- [1] Pflanz, H.M.J. Steady state and transient properties of electric arcs. Thesis Eindhoven, (1967).
- [2] Hermann, W. Zs. für Phys. 216 (1968) 33.
- [3] Morris, J.C. and Rudis, R.P. and Yos, J.M. Phys. of Fluids 13 (1970) 608.
- [4] Zel'dovich, Ya.B. and Raizer, Yu. P. Physics of shock waves and high temperature hydrodynamic phenomena. Volume I. Academic Press New York (1966). p. 128.
- [5] Chandrasekhar, S. Radiative transfer. Dover publications Inc., New York, (1960). p.8.
- [6] Kramers, H.A. Phil. Mag. 46 (1920) 836.
- [7] Zel'dovich, Ya.B and Raizer, Yu. P. Loc. cit [4] p. 259.
- [8] Griem, H.R. Plasma spectroscopy Mc.Graw-Hill Book Co., New York, (1964). p. 112.
- [9] Zel'dovich, Ya.B. and Raizer Yu. P. Loc cit. [4] p. 269.
- [10] Unsöld, A. Ann. der Physik 33 (1938) 607.
- [11] Meacker, H. and Peters, T. Zs. für Phys. 139 (1954) 448.
- [12] Vitense, E. Zs. für Astrophys. 28 (1951) 81.
- [13] Unsöld, A. Physik der Sternatmosphären. Springer Verlag, Berlin, (1968). p. 288.
- [14] Baranger, M. and Bates, D.R. (editor) Atomic and Molecular Processes. Academic Press, New York, (1962). p. 493.
- [15] Griem, H.R. Loc cit. [8] p. 63.
- [16] Griem, H.R. Loc cit. [8] table 4 - 5, p. 454 and table 4 - 6, p. 557.
- [17] Griem, H.R. Loc cit. [8] p. 90.
- [18] Griem, H.R. Loc cit. [8] p. 101.
- [19] Unsöld, A. Loc cit. [13] p. 261.
- [20] Hulst, H.C. v.d. and Reesinck, J.J.M. Bull. Astr. Netherlands 9 (1941) 225.

- [21] Posener, D.W. Austr. Journ. Phys. 12 (1959) 184.
- [22] Vries, R.F. de Rijnhuizen report (65-26) (Euratom-FOM) (1965).
- [23] Herzberg, G. Atomic spectra and atomic structure. Dover publications, New York, (1944). p. 144..
- [24] Wiese, W.L., Smith, M.W. and Glennon, B.M. Atomic transition probabilities Volume I Hydrogen through Neon. National Bureau of Standards, Washington DC , (1966).
- [25] Pflanz, H.M. and Horst, D.Th. Particle densities of high temperature gases. (Hydrogen, Nitrogen, Oxygen). J. ter Report T.H. Eindhoven. Dept. of Electrical Engineering, Group High Voltage - High Currents (1966).
- [26] Andriessen, F.J. High current discharges in a forced gas flow. Thesis Eindhoven, (1973). Loc. cit 8 p. 454.
- [27] Griem, H.R. J. Soc. Indust. Appl. Math. 5 (1957) 74.
- [28] Forsythe, G.E. Num. Mathem. 6 (1964) 413.
- [29] Bulirsch, R. and Stoer, J. Num. Mathem. 3 (1961) 285.
- [30] Stoer, J. Optics and spectroscopy 16 (1964) 96.
- [31] Vorobyov, V.S. and Norman, G.E. Private communication.
- [32] Uhlenbusch, J. Radiative energy transport in arcs. Proc. int. conf. pehn. ion gases. London, 1971. p. 176.
- [33] Hermann, W. and Schade, E.

```

Lalgol 06265097 boerman,1
begin real g, bb, theta;
  integer i;
  array d, e[1:4];
  library INTEGRAL, ARCCOS;
  real procedure B(g);
  value g; real g;
  begin real hulp, grens;
    if g = 0 then B := arctan(1) × 2
      else begin grens := ARCCOS(g/(14.85 + g - ln(ARCCOS(g/(g + 2.3)))));
        hulp := exp(-g);
        B := hulp × INTEGRAL(theta, exp(-g/cos(theta))/hulp, 0, grens, d, e, false, false)
      end
    end B;

  e[1] := e[3] := n-5; e[2] := n-7; e[4] := 0;
  RUNOUT;
  for i := 0 step 1 until 1500 do
  begin g := i × n-2; bb := B(g);
    ABSFIXT(2, 2, g); FLOT(10, 1, bb); NLCR;
    FIXP(2, 2, g); PUNCH(bb); PUNLCR
  end;
  RUNOUT
end
progend

```

APPENDIX II.

Text of the programme for the calculation of the contribution of a spectral line to the radiative balance in the axis of a discharge.

The sequence of the input data.

1. Number of temperature data in the $T(r)$ table.
2. Number of temperature data in the $n_N(T)$ c.q. $n_{N+}(T)$; $U(T)$ and $n_e(T)$ tables.
3. The $n_N(T)$ c.q. $n_{N+}(T)$; $U(T)$ and $n_e(T)$ tables.
4. The values of the constants λ_{mj} , I_j ; g_j ; f_{jm} and w_{tab} .
5. The exponential integral $B(g)$ as a function of g .
6. The $T(r)$ table.

Output data.

See programme text.

```

Lalgol06265097 boerman
begin comment W.BUERMAN,T.H.E. 7/71,
straling van boogontlading in het centrum,
ingevoerd worden achtereenvolgens:
1.aantal T(r) waarden,
2.aantal (T,n-u,u-n,n-e) waarden,
3.tabel (T,n-u,u-n,n-e),
4.lambda,e-i,g,i,f-ik,wtabel,
5.in 1500 waarden tabel: g, B(g) om en om,
6.in opgegeven aantal waarden tabel: r, T om en om
N.B. de laatste waarde van deze tabel wordt als boogradius beschouwd;

integer TOP,RARMAX,MAX,gi;
real LAMBDA,NUO,NU,EI,DELTA NU,pi,p,h,k,c,e2mc4eps,f1k,kfaktor,hnugedk,eigedk,ALFAKTOR,EPSFAKTOR,
a,WINLES,EXTRA,BEIFAKTOR,BRO,pibro;
RARMAX := READ; MAX := READ;
pi := 4 x arctan(1);
h := 6.624n-34;
k := 1.38n-23;
c := 2.998n+8;
e2mc4eps := .25565n-5;

begin real ENU, ENU1, ANU, UNU, RQ, fi, RADIUS, R, T, theta, m, n, minr, ALFA, RQMIN, RQMAX, stukanu;
integer i, I, J, nne, nnu, d, e;
real array RAR, TRAR[1:RARMAX],
UAR, BAR, FAR, alphae, alphau, betae, betau[1:MAX],
ae, au[0:MAX], delta[-1:MAX],
GAR, BAR[0:1500],
UITVOER[0:3, 1:2C];
library ORTHOFOL, YAPPROX;

real procedure TRAPEX (x, fx, a, b, ae, re, orde, m);
value a, b, re, ae; integer orde, m; real x, fx, a, b, ae, re;
begin comment De procedure TRAPEX geeft een benadering van de waarde van de integraal van de functie f(x) over het
interval [a, b]. De procedure benadert deze waarde door extrapolaties van rationale functies, gebaseerd
op het berekenen van een aantal trapezium-benaderingen. Bij aanroep van de procedure moet de formele parameter
fx vervangen worden door de expressie voor f(x). x treedt op als Jensen parameter. Het maximale aantal
trapezium-benaderingen moet aan de procedure meegegeven worden met de integer orde. Het proces eindigt als
door twee opeenvolgende extrapolaties T[m], T[m - 1] voldaan is aan abs(T[m - 1] - T[m]) ≤ ae + re x abs(T[m])
of als m de waarde orde heeft bereikt. Na afloop van de procedure heeft m als waarde het aantal
berekende trapezium-benaderingen of, indien niet aan de eindtest voldaan kan worden, de waarde nul;

integer nn, i; real f1, f2, f2a, f3, h0, h, to, tr, tn;
integer array n[0:orde]; array t[0:];
procedure extr (m); value m; integer m;
begin integer i, mm; real u, v, tu, tv, d;
v := 0; u := t[0]; tr := t[0] := tu; if m > 7 then mm := 7 else mm := m;
for i := 1 step 1 until mm do
begin d := n[i]/n[i - 1]; d := d x d; tv := tr - v; tu := tr - u;
if tv ≠ 0 then tr := tr + tu/(d x (1 - tu/tv) - 1);
if i ≠ mm then begin v := u; u := t[i] end; t[i] := tr;
end
end extr;

```

```

n[0] := 1; n[1] := 2; n[2] := 3; for i := 3 step 1 until orde do n[i] := n[i - 2] × 2 ;
h0 := b - a; x := a; f1 := fx; UITVOER[d, e] := 4 × pi × f1; x := b; f1 := (f1 + fx)/2; t[0] := f1 × h0;
x := a + h0/2; f2a := f2 := fx; UITVOER[d, e + 1] := 4 × pi × f2;
if d = 1 then begin UITVOER[0, e] := a; UITVOER[0, e + 1] := x; e := e + 2 end;
tn := (f1 + f2) × h0/2; extr(1); to := tr;
for m := 2 step 1 until orde do
begin if m = 2 then begin x := a + h0/3; f3 := fx; x := b - h0/3; f3 := f3 + fx; tn := (f1 + f3) × h0/3 end
      else begin nn := n[m]; h := h0/nn;
              if m = (m : 2) × 2
              then begin for i := 1 step 6 until nn, 5 step 6 until nn do
                        begin x := a + i × h; f3 := f3 + fx end;
                        tn := (f3 + f2a + f1) × h; f2a := f2
                        end
              else begin for i := 1 step 2 until nn do begin x := a + i × h; f2 := f2 + fx end;
                        tn := (f2 + f1) × h
                        end
              end;
      extr(m); if abs(to - tr) ≤ ae + re × abs(tr) then goto end else to := tr
end;
m := 0;
end: TRAPEX := tr
end TRAPEX;

real procedure INTEGRAND(a);
value a; real a;
begin real alp0, alpi, alpi1, eps, hsug, g, var, som1, som2;
integer i;
array INTAR[0:100];
alp0 := alp0 := ALPHANU(0); eps := alp0 × EPSFAKTOR × exp(-hnugedk/T);
hsug := 15/alp0; if hsug > RADIUS then hsug := RADI S; hsug := hsug/100.001;
g := 0; INTAR[0] := BAR[0] × eps;
for i := 1 step 1 until 100 do
begin var := i × hsug;
alp1 := ALPHANU(var); eps := alpi1 × EPSFAKTOR × exp(-hnugedk/T);
g := g + .5 × hsug × (alpi + alpi1);
INTAR[i] := B(g) × eps;
alpi := alpi1
end;
som1 := 0; som2 := 0;
for i := 1 step 2 until 99 do som1 := som1 + INTAR[i];
for i := 2 step 2 until 98 do som2 := som2 + INTAR[i];
INTEGRAND := hsug × (INTAR[0] + INTAR[100] + 4 × som1 + 2 × som2)/3
end INTEGRAND;

```

```

real procedure EPSILONU(R);
value R;real R;
begin EPSILONU:=ALPHANU(R)×EPSFAKTOR×exp(-hnugedk/T);
end EPSILONU;

```

```

real procedure ALPHANU(R);
value R;real R;
begin real BETA,BETAFAKTOR;
      RT(R,T);
      BETA:=BETFAKTOR×YAPPROX(nme,alphae,betae,ae,T);
      BETAFAKTOR:=BETA×(1+(α×BRO/BETA)2);
      EXTRA:=ALFAKTOR×(exp(-eigedk/T))×YAPPROX(nnu,alphau,betau,au,T)/BETAFAKTOR;
      ALPHANU:=EXTRA;
end ALPHANU;

```

```

procedure RT(R,T);
value R;real R,T;
begin integer og,mg,bg;
      og:=1;bg:=RARMAX;
V:    mg:=og+((bg-og):2);
      if R<RAR[mg] then bg:=mg else og:=mg;
      if (bg-og)>1.5 then goto V;
      T:=(TRAR[bg]-TRAR[og])×(R-RAR[og])/(RAR[bg]-RAR[og])+TRAR[og]
end RT;

```

```

real procedure B(g);
value g;real g;
begin integer og, mg, bg;
      if g > 15 then begin B := 0; goto eindbg end;
      og := 0; bg := 1500;
V:    mg := og + ((bg - og) : 2);
      if g ≤ GAR[mg] then bg := mg else og := mg;
      if (bg - og) > 1.5 then goto V;
      B := (BAR[bg] - BAR[og]) × (g - GAR[og]) / (GAR[bg] - GAR[og]) + BAR[og];
      eindbg: ;
end B;

```

```

real procedure EEN(a);
value a;real a;
begin NU:=NUO+aXBRO;
      hnagedk:=hXNU/k;EPSTFAKTOR:=2XhXNUMXNUXNU/(cxc);
      EEN:=1
end EEN;
for I:=1 step 1 until MAX do
begin TAR[I]:=READ;UAR[I]:=READ/READ;EAR[I]:=READ
end;
LAMBDA := READ; EI := READ; gi := READ; fik := READ; WINLEES := READ; NUO := c/LAMBDA;
PRINTTEXT(⟨de invoergegevens zijn:⟩); CARRIAGE(2);
PRINTTEXT(⟨      lambda=⟩); FLOT(6, 2, LAMBDA); PRINTTEXT(⟨ meter⟩); NLCR;
PRINTTEXT(⟨      nu=0 =>⟩); FLOT(6,2, NUO); PRINTTEXT(⟨ hertz⟩); NLCR;
PRINTTEXT(⟨      ei   =>⟩); FIXT(5, 0, EI); PRINTTEXT(⟨ /cm⟩); NLCR;
PRINTTEXT(⟨      gi   =>⟩); FIXT(5, 0, gi); NLCR;
PRINTTEXT(⟨      fik  =>⟩); FIXT(1, 4, fik); NLCR;
PRINTTEXT(⟨      wtabel=⟩); FLOT(6, 2, WINLEES); PRINTTEXT(⟨ meter⟩); NLCR;
for I := 0 step 1 until 1500 do begin GAR[I] := READ; BAR[I] := READ end;
for I:=1 step 1 until RARMAX do begin RAR[I]:=READXn-3;TRAR[I]:=READ end;
RADIUS:=RAR[RARMAX];
ORTHOPOL(TAR,UAR,MAX,nnu,MAX-1,alphau,betau,au,delta,delta[nmu]/delta[-1]≤n-8);
ORTHOPOL(TAR,EAR,MAX,nne,MAX-1,alphae,betae,ae,delta,delta[nne]/delta[-1]≤n-6);
BETFAKTOR:=2.998n-14XWINLEES/(LAMBDA2);
T := TRAR[1]; BRO := BETFAKTOR X YAPPROX(nne, alphae, betae, ae, T);
pibro:=8XpiXBRO;
elgedk:=1.43855XEI;ALFAKTOR:=e2mc4epsXgiXfik/pi;
PRINTTEXT(⟨      RADIUS=⟩); FLOT(6, 2, RADIUS); PRINTTEXT(⟨ meter⟩); CARRIAGE(3);
PRINTTEXT(⟨kenkele ingelezen en verwerkte waarden⟩); CARRIAGE(2);
PRINTTEXT(⟨      r      t      ne⟩); NLCR;
PRINTTEXT(⟨      mm      kelvin      mK-3⟩); NLCR;
SPACE(6); for I := 1 step 1 until 25 do PRSYM(65); NLCR;
for I := 0 step 1 until 10 do
begin SPACE(5); ABSFIXT(1, 2, I X RADIUS X n+2);
      RT(I X RADIUS/10, T); ABSFIXT(5, 1, T);
      FLOT(5, 2, YAPPROX(nne, alphae, betae, ae, T)); NLCR
end;
CARRIAGE(3);
PRINTTEXT(⟨kenkele nuttige gegevens⟩); CARRIAGE(2);
PRINTTEXT(⟨      de orden der benaderingspolynomen zijn: ⟩);
FIXT(2, 0, nnu); FIXT(2, 0, nne); NLCR;
PRINTTEXT(⟨      de halfhalfwaardebreedte bedraagt ⟩);
FLOT(6, 2, BRO); PRINTTEXT(⟨ hertz⟩); CARRIAGE(2);
PRINTTEXT(⟨      1/alphanu(0) als functie van de frequentieafwijking⟩); NLCR;
PRINTTEXT(⟨      a      1/alphanu(0)⟩); NLCR;
for a := 0, .5, 1, 2, 3, 6.5, 10, 20, 30, 65, 100, 200, 300, 650, 1000 do
begin SPACE(8); ABSFIXT(4, 1, a); FLOT(6, 2, 1/ALPHANU(0)); NLCR end;

```



```

begin integer amin,amax;
  amin:=1;ANU:=0;ENU:=0;
  NEW PAGE; e := 1;
  d := 2; TRAPEX(a, EEN(a) × ALPHANU(0) × INTEGRAND(a), 0, 1, 0,  $\pi^4$ , 2, TOP);
  d := 1; ENU1 := TRAPEX(a, EEN(a) × EPSILONU(0), 0, 1, 0,  $\pi^4$ , 10, TOP);
  ABSFIXT(3, 0, LINE NUMBER);PRINTTEXT(amin,amax, en m in enu zijn achtereenvolgens  });
  ABSFIXT(4, 0, 0); ABSFIXT(4, 0, 1); ABSFIXT(2, 0, TOP); NLCR;
  for amax:=3,10,30,100,300,1000 do
  begin ABSFIXT(3,0,LINE NUMBER);
    PRINTTEXT(amin,amax,m in anu, en m in enu zijn achtereenvolgens});
    ABSFIXT(4,0,amin);ABSFIXT(4,0,amax);
    d := 2;
    ANU := ANU + TRAPEX(a, EEN(a) × ALPHANU(0) × INTEGRAND(a), amin, amax, 0,  $\pi^4$ , 10, TOP);
    ABSFIXT(3,0, TOP);
    d := 1;
    ENU:=ENU+TRAPEX(a,EEN(a)×EPSILONU(0),amin,amax,0, $\pi^4$ ,10,TOP);
    ABSFIXT(3,0,TOP);NLCR;
    amin:=amax
  end;
  UNU := ENU - ANU; CARRIAGE(5);
  PRINTTEXT(UNU=);FLOT(5,2,pibro×UNU);NLCR;
  ENU := ENU + UNU;
  PRINTTEXT(ANU=); FLOT(5, 2, pibro × ANU); NLCR;
  PRINTTEXT(ENU=);FLOT(5,2,pibro×ENU);
  NLCR;PRINTTEXT(UNU is);FIXT(2,2,UNU/ENU×100);PRINTTEXT(procent van enu);
end;
begin for I := 1 step 1 until e - 1 do UITVOER[3, I] := UITVOER[1, I] - UITVOER[2, I];
  CARRIAGE(5);
  PRINTTEXT(a enu anu unu); NLCR;
  for I := 1 step 1 until e - 1 do
  begin ABSFIXT(3, 1, UITVOER[0, I]); FLOT(5, 3, UITVOER[1, I]); FLOT(5, 3, UITVOER[2, I]);
    FLOT(5, 3, UITVOER[3, I]); NLCR
  end
end;
end;
end;
EIND;
end
progend
3

```

APPENDIX III.

Text of the programme for the calculation of the contribution of a spectral line to the radiative balance in points out of the axis of a discharge.

The sequence of the input data.

1. Number of temperature data in the $T(r)$ table.
2. Number of temperature data in the $n_N(T)$ c.q. $n_{N+}(T)$; $U(T)$ and $n_e(T)$ tables.
3. The magnitudes of staptal and staptal 1.
4. The $n_N(T)$ c.q. $n_{N+}(T)$; $U(T)$ and $n_e(T)$ tables.
5. The line identifier and the magnitude of r_A .
6. The values of the constants g_j , I_j , f_{jm} , λ_{mj} and w_{tab} .
7. The exponential integral $B(g)$ as a function of g .
8. The $T(r)$ table.

Output data.

See programme text.

lalgol 06265238 holtz

begin comment Berekening van straling in een boogontlading voor punten buiten de as. 11-71 T.H.E.

Inlees volgorde: aantal waarden van t in t(r) tabel,
aantal waarden van t in tabel 2.
de waarden van staptal en staptal1,
de waarden van t,un,un,ne uit tabel 2,
de lijn identifier en de waarde van ra,
de waarden van de constanten g1, ei, fik, lambda, wtab,
de waarden van g en b(g) uit b(g) tabel,
de waarden van t en r uit t(r) tabel.;

integer numberr, numbertr, rij, kolom; real array tabel[0:3, 1:20];

numbertr := read; numberr := read;

begin real g1,ei,fik,lambda0,theta,r,wtab,pi,c,alphafaktor,t,a,ra,betalra,alphara,enu,ara,nu0,
alpharq,

rs, rq, epsfaktor1, epsfaktor2, radius, lnu, fi, fimax, rmin, rmax, smax;

integer i, nun, nne, staptal, staptal1, lijn;

real array un,ne,tt[1:numberr],alphaun,betaun,alphane,betane[1:numberr - 1],aun,ane[0:numberr - 1],
delta[-1:numberr - 1], tr, rr[1:numbertr], be, gg[0:1000];

library ORTHOPOL,YAPPROX;

real procedure TRAPEX (x, fx, a, b, ae, re, orde, m);

value a, b, re, ae, orde; integer orde, m; real x, fx, a, b, ae, re;

begin comment De procedure TRAPEX geeft een benadering van de waarde van de integraal van de functie f(x) over het interval [a, b]. De procedure benadert deze waarde door extrapolaties van rationale functies, gebaseerd op het berekenen van een aantal trapezium-benaderingen. Bij aanroep van de procedure moet de formale parameter fx vervangen worden door de expressie voor f(x). x treedt op als Jensen parameter. Het maximale aantal trapezium-benaderingen moet aan de procedure meegegeven worden met de integer orde. Het proces eindigt als door twee opeenvolgende extrapolaties T[m], T[m - 1] voldaan is aan $\text{abs}(T[m - 1] - T[m]) \leq ae + re \times \text{abs}(T[m])$ of als m de waarde orde heeft bereikt. Na afloop van de procedure heeft m als waarde het aantal berekende trapezium-benaderingen of, indien niet aan de eindtest voldaan kan worden, de waarde nul;

integer mn, i; real f1, f2, f2a, f3, h0, h, to, tr, tn;

integer array n[0:orde]; array t[0:7];

procedure extr (m); value m; integer m;

begin integer i, mm; real u, v, tu, tv, d;

v := 0; u := t[0]; tr := t[0] := tn; if m > 7 then mm := 7 else mm := m;

for i := 1 step 1 until mm do

begin d := n[m]/n[m - 1]; d := d × d; tv := tr - v; tu := tr - u;

if tv ≠ 0 then tr := tr + tu/(d × (1 - tu/tv) - 1);

if i ≠ mm then begin v := u; u := t[i] end; t[i] := tr;

end

end extr;

n[0] := 1; n[1] := 2; n[2] := 3; for i := 3 step 1 until orde do n[i] := n[i - 2] × 2;

h0 := b - a; x := a; f1 := fx; tabel[kolom, rij] := f1;

x := b; f1 := (f1 + fx)/2; t[0] := f1 × h0;

x := a + h0/2; f2a := f2 := fx; tabel[kolom, rij + 1] := f2;

if kolom = 1 then begin tabel[0, rij] := a; tabel[0, rij + 1] := x; rij := rij + 2 end;

tn := (f1 + f2) × h0/2; extr(1); to := tr;

for m := 2 step 1 until orde do

begin if m = 2 then begin x := a + h0/3; f3 := fx; x := b - h0/3; f3 := f3 + fx; tn := (f1 + f3) × h0/3 end

```

else begin mn := n[m]; h := h0/mn;
      if m = (m : 2) * 2
      then begin for i := 1 step 6 until mn, 5 step 6 until mn do
                begin x := a + i * h; f3 := f3 + fx end;
                tn := (f3 + f2a + f1) * h; f2a := f2
              end
            else begin for i := 1 step 2 until mn do begin x := a + i * h; f2 := f2 + fx end;
                tn := (f2 + f1) * h
              end
            end;
      extr(m); if abs(to - tr) < ae + re * abs(tr) then goto end else to := tr
    end;
  m := 0;
end: TRAPEX := tr
end TRAPEX;

```

```

real procedure beta1(t);
value t; real t;
begin beta1 := c * wtab * n-22 * YAPPROX( nne, alphane, betane, ane ,t)/lambda0 2;
end beta1;

```

```

real procedure alpha(r);
value r; real r;
begin real betat;
  t := temp(r); betat := beta1(t);
  alpha := alphafaktor * YAPPROX(nun,alphaun,betaun,aun,t) * betat/(betat 2 + (a * beta1ra) 2)
  * exp((- 1.43855 * ei)/t)
end alpha(r);

```

```

real procedure een(a);
value a; real a;
begin real nu;
  nu := nu0 + a * beta1ra;
  epsfaktor1 := 2 * 6.624n-34 * nu 3/c 2;
  epsfaktor2 := 6.624n-34 * nu/1.38n-23;
  een := 1;
end een;

```

```

real procedure epsilon(r);
value r; real r;
begin alharq := alpha(r); epsilon := alharq * epsfaktor1 * exp(- epsfaktor2/t)
end epsilon(r);

```

```

real procedure temp(r);
value r; real r;
begin integer og, mg, bg;
  og := 1; bg := numbertr;
V:  mg := og + ((bg - og) : 2);
  if r < rr[mg] then bg := mg else og := mg;
  if (bg - og) > 1.5 then goto V;
  temp := (tr[bg] - tr[og]) * (r - rr[og])/(rr[bg] - rr[og]) + tr[og];
end temp(r);

```

```

real procedure simpson(x, fx, a, b, step);
value a, b, step; real a, b, x, fx; integer step;
begin real array fxar[0:step];
      real h, som1, som2;
      integer ii;
      h := (b - a)/step;
      for ii := 0 step 1 until step do begin x := a + ii × h; fxar[ii] := fx end;
      som1 := som2 := 0;
      for ii := 1 step 2 until step - 1 do som1 := som1 + fxar[ii];
      for ii := 2 step 2 until step - 2 do som2 := som2 + fxar[ii];
      simpson := h/3 × (fxar[0] + 4 × som1 + 2 × som2 + fxar[step]);
end simpson;

real procedure b(rq);
value rq; real rq;
begin real g, s; integer og, mg, bg;
      s := sqrt(ra 2 + rq 2 - 2 × ra × rq × cos(fi)); g := s/2 × (alphara + alpharq);
      if g = 0 then b := 0 else
      begin if g > 10 then b := 0 else
            begin og := 0; bg := 1000;
                  V: mg := og + ((bg - og) : 2);
                     if g < gg[mg] then bg := mg else og := mg;
                     if (bg - og) > 1.5 then goto V;
                     b := ((be[bg] - be[og]) × (g - gg[og]) / (gg[bg] - gg[og]) + be[og]) / (s + n-2 × lnu);
            end;
      end;
end b(rq);

real procedure anu(a);
value a; real a;
begin een(a);
      alphara := alpha(ra);
      smax := 10/alphara;
      rmin := ra - smax; if rmin < 0 then rmin := 0;
      rmax := ra + smax; if rmax > radius then rmax := radius;
      if smax > ra then fimax := pi else fimax := arctan(smax/sqrt(ra 2 - smax 2));
      rs := anu := 4 × alphara ×
      ( simpson(rq, epsilon(rq) × rq × simpson(fi, b(rq), 0, fimax, staptal), rmin, (4 × ra + rmin)/5, staptal)
      + simpson(rq, epsilon(rq) × rq × simpson(fi, b(rq), 0, fimax/5, staptal1), (4 × ra + rmin)/5, (4 × ra + rmax)/5, staptal1)
      + simpson(rq, epsilon(rq) × rq × simpson(fi, b(rq), fimax/5, fimax, .8 × staptal),
              (4 × ra + rmin)/5, (4 × ra + rmax)/5, staptal/5)
      + simpson(rq, epsilon(rq) × rq × simpson(fi, b(rq), 0, fimax, staptal), (4 × ra + rmax)/5, rmax, staptal));
end anu(a);
staptal := read; staptal1 := read;
pi := 3.14159 26535; c := 2.998n+8;
for i:=1 step 1 until numbert do
begin tt[i] := read; un[i] := read/read; ne[i] := read end;
ORTHOPOL(tt, un, numbert, nun, numbert - 1, alphaun, betaun, aun, delta, delta[nun]/delta[-1] <= n-6);
ORTHOPOL(tt, ne, numbert, nne, numbert - 1, alphane, betane, ane, delta, delta[nne]/delta[-1] <= n-6);

```

```

lijn := read; ra := read;
gi := read; ei := read; fik := read; lambda0 := read; wtab := read;
for i := 0 step 1 until 1000 do
begin gg[i] := read; be[i] := read end;
for i := 1 step 1 until numbertr do
begin rr[i] := read * n-3; tr[i] := read end;
alphafaktor := 0.26565 * n-5 * gi * fik/pi;
nu0 := c/lambda0; radius := rr[numbertr];
beta1ra := beta1(temp(ra)); a := 0; lnu := 1/alpha(ra);
PRINTTEXT(⟨de invoergegevens zijn:⟩); CARRIAGE(2);
PRINTTEXT(⟨deze gegevens behoren bij lijn: n⟩); PRSYM(lijn : 1000); lijn := lijn - 1000 * (lijn : 1000);
if lijn > 99 then PRINTTEXT(⟨som ad⟩); ABSFIXT(2,0,lijn - 100 * (lijn : 100)); NLCR;
PRINTTEXT(⟨lambda=⟩); FLOT(6, 2, lambda0); PRINTTEXT(⟨ meter⟩); NLCR;
PRINTTEXT(⟨ nu-0 =⟩); FLOT(6, 2, c/lambda0); PRINTTEXT(⟨ hertz⟩); NLCR;
PRINTTEXT(⟨ ei =⟩); FIXT(5, 0, ei); PRINTTEXT(⟨ /cm⟩); NLCR;
PRINTTEXT(⟨ gi =⟩); FLOT(3, 1, gi); NLCR;
PRINTTEXT(⟨ fik =⟩); FLXT(1, 4, fik); NLCR;
PRINTTEXT(⟨ wtabel=⟩); FLOT(6, 2, wtab); PRINTTEXT(⟨ meter⟩); NLCR;
PRINTTEXT(⟨ ra =⟩); ABSFIXT(1, 2, ra * n+3); PRINTTEXT(⟨ mm⟩); NLCR;
PRINTTEXT(⟨ t(ra) =⟩); ABSFIXT(5, 1, temp(ra)); PRINTTEXT(⟨ kelvin⟩); NLCR;
PRINTTEXT(⟨ radius=⟩); FLOT(6, 2, radius); PRINTTEXT(⟨ meter⟩); NLCR;
PRINTTEXT(⟨ 1-nu =⟩); FLOT(6, 2, lnu); PRINTTEXT(⟨ meter⟩); NLCR;
CARRIAGE(2); PRINTTEXT(⟨ enkele ingelezen en verwerkte waarden⟩); CARRIAGE(2);
PRINTTEXT(⟨ r t ne n/u ⟩); NLCR;
PRINTTEXT(⟨ mm kelvin mA-3 ⟩); NLCR;
SPACE(6); for i := 1 step 1 until 37 do PRSYM(65); NLCR;
for i := 1 step 1 until 10 do
begin SPACE(5); ABSFIXT(1, 2, i * radius * 100);
ABSFIXT(5, 1, temp(i * radius/10));
FLOT(5, 2, YAPPROX(nne, alphane, betane, ane, temp(i * radius/10)));
FLOT(5, 2, YAPPROX(nun, alphaun, betaun, aun, temp(i * radius/10))); NLCR;
end;
CARRIAGE(3);
PRINTTEXT(⟨ enkele nuttige gegevens⟩); CARRIAGE(2);
PRINTTEXT(⟨ de orden van de benaderingspolynomen zijn:⟩);
ABSFIXT(2, 0, nun); ABSFIXT(2, 0, nne); NLCR;
PRINTTEXT(⟨ de half-half-waardebreedte bedraagt⟩);
FLOT(6, 2, beta1ra); PRINTTEXT(⟨ hertz⟩); NLCR;
NLCR; PRINTTEXT(⟨ 1/alphanu(ra) als functie van de frequentieafwijking a⟩); NLCR;
PRINTTEXT(⟨ a 1/alphanu(ra)⟩); NLCR;
for a := 0, .5, 1, 2, 3, 6.5, 10, 20, 30, 65, 100, 200, 300, 650, 1000 do
begin SPACE(3); ABSFIXT(4, 1, a); FLOT(6, 2, 1/alpha(ra)); NLCR end;
begin integer amin, amax, top; real enu1, pi4, unu, aanu;
amin := 2; aanu := enu := 0; pi4 := 4 * pi;
NEWPAGE; rij := 1;
kolom := 2; TRAPEX(a, anu(a), 0, 2, 0, n-4, 2, top);
kolom := 1; enu1 := TRAPEX(a, een(a) * pi4 * epsilon(ra), 0, 2, 0, n-4, 7, top);
ABSFIXT(3,0,LINE NUMBER); PRINTTEXT(⟨ amin, amax, en m in enu zijn: ⟩);
SPACE(10); ABSFIXT(4, 0, 0); ABSFIXT(4, 0, 2); ABSFIXT(3, 0, top); NLCR;

```

```

for amax := 3, 10, 30, 100, 300, 1000 do
begin ABSFIXT(3,0,LINE NUMBER);
PRINTTEXT(amin, amax, m in anu en m in enu zijn: );
ABSFIXT(4,0,amin); ABSFIXT(4,0,amax);
kolom := 2;
aanu := aanu + TRAPEX(a, anu(a), amin, amax, 0, n-3, 7, top);
ABSFIXT(3,0,top);
kolom := 1;
enu := enu + TRAPEX(a, een(a) × pi4 × epsilon(ra),amin, amax, 0, n-4, 10, top);
ABSFIXT(3,0,top); NLCR;
amin := amax;

end;
unu := enu - aanu; CARRIAGE(5);
PRINTTEXT(unu); FLOT(8,2,2 × beta1ra × unu); NLCR;
enu := enu + unu;
PRINTTEXT(anu); FLOT(8,2, 2 × beta1ra × aanu); NLCR;
PRINTTEXT(enu); FLOT(8,2, 2 × beta1ra × enu); NLCR;
PRINTTEXT(unu is); FIXT(2,2,unu/enu × 100); PRINTTEXT(procent van enu);
for i := 1 step 1 until rij - 1 do tabel[3,i] := tabel[1,i] - tabel[2,i];
CARRIAGE(5);
PRINTTEXT(a enu anu unu); NLCR;
for i := 1 step 1 until rij - 1 do
begin ABSFIXT(3,1,tabel[0,i]); FLOT(5,3,tabel[1,i]); FLOT(5,3,tabel[2,i]);
FLOT(5,3,tabel[3,i]); NLCR;
end;
end;
end;
end
progend
371 7
30 30;
9000 .22175n+25 4.52220 1.19n+22
10000 .20398n+25 4.72381 3.12n+22
12000 .15255n+25 5.18927 1.24n+23
14000 .93841n+24 5.71250 2.92n+23
16000 .43159n+24 6.28290 4.50n+23
18000 .15756n+24 6.91593 5.13n+23
20000 .55652n+23 7.65386 5.05n+23

```

APPENDIX IV.

Text of the programme for the calculation of the contribution to the radiative balance of the bound-free continuum ($h\nu > I$) to the radiative balance in the axis of a discharge.

The sequences of the input data.

1. Number of temperature data in the $T(r)$ table.
2. Number of temperature data in the $n_N(T)$ table.
3. The value for v_{\max} .
4. The value for Z^{*2} .
5. The $n_N(T)$ table.
6. The exponential integral $B(g)$ as a function of g .
7. The $T(r)$ table.

Output data.

See programme text.

Lalcol06265097 BOERMAN

begin comment W. BOERMAN, T.H.E. 7/71

straling van boogontlading in het centrum;

APENDIX IV-II.

integer TOP, RARMAX, MAX, Z2;
real NUO, NU, NUMAX, pi, h, k, c, hmgedk, EPSFAKTOR, a, BRO, pibro;
RARMAX:=READ; MAX:=READ;
NUMAX := READ; NUO := 3.5_n+15; Z2 := READ;
PRINTTEXT($\sqrt{z^2 - 1}$); ABSFIXT(2,0,Z2); NLCR;

pi:=4*arctan(1);
h:=6.624_n-34;
k:=1.38_n-25;
c:=2.998_n+8;

begin real ENU, ANU, UNU, RQ, RADIUS, R, T;
integer i, j, J, nne, nnu, d, e;
real array RAR, TRAR[1:RARMAX],
UAR, EAR, TAR, alphae, alphau, betae, betau[1:MAX],
ae, au[0:MAX], delta[-1:MAX],
GAR, BAR[0:1500],
UITVOER[0:3, 1:20];
library ORTHOPOL, YAPPROX;

real procedure TRAPEX (x, fx, a, b, ae, re, orde, m);

value a, b, re, ae, orde; integer orde, m; real x, fx, a, b, ae, re;

begin comment De procedure TRAPEX geeft een benadering van de waarde van de integraal van de functie f(x) over het interval [a, b]. De procedure benadert deze waarde door extrapolaties van rationale functies, gebaseerd op het berekenen van een aantal trapezium-benaderingen. Bij aanroep van de procedure moet de formele parameter fx vervangen worden door de expressie voor f(x). x treedt op als Jensen parameter. Het maximale aantal trapezium-benaderingen moet aan de procedure meegegeven worden met de integer orde. Het proces eindigt als door twee opeenvolgende extrapolaties T[m], T[m-1] voldaan is aan $\text{abs}(T[m-1] - T[m]) \leq \text{ae} + \text{re} \times \text{abs}(T[m])$ of als m de waarde orde heeft bereikt. Na afloop van de procedure heeft m als waarde het aantal berekende trapezium-benaderingen of, indien niet aan de eindtest voldaan kan worden, de waarde nul;

integer mm, i; real f1, f2, f2a, f3, h0, h, to, tr, tn;

integer array n[0:orde]; array t[0:7];

procedure extr (m); value m; integer m;

begin integer i, mm; real u, v, tu, tv, d;
v := 0; u := t[0]; tr := t[0] := tn; if m > 7 then mm := 7 else mm := m;
for i := 1 step 1 until mm do
begin d := n[m]/n[m-1]; d := d x d; tv := tr - v; tu := tr - u;
if tv ≠ 0 then tr := tr + tu/(d x (1 - tu/tv) - 1);
if i ≠ mm then begin v := u; u := t[i] end; t[i] := tr;

end

end extr;

```

n[0] := 1; n[1] := 2; n[2] := 3; for i := 3 step 1 until orde do n[i] := n[i - 2] × 2 ;
h0 := b - a; x := a; f1 := fx; UITVOER[d, e] := 4 × pi × f1; x := b; f1 := (f1 + fx)/2; t[0] := f1 × h0;
x := a + h0/2; f2a := f2 := fx; UITVOER[d, e + 1] := 4 × pi × f2;
if d = 1 then begin UITVOER[0, e] := a; UITVOER[0, e + 1] := x; e := e + 2 end;
tn := (f1 + f2) × h0/2; extr(1); to := tr;
for m := 2 step 1 until orde do
begin if m = 2 then begin x := a + h0/3; f3 := fx; x := b - h0/3; f3 := f3 + fx; tn := (f1 + f3) × h0/3 end
      else begin nn := n[m]; h := h0/nn;
              if m = (m : 2) × 2
              then begin for i := 1 step 6 until nn, 5 step 6 until nn do
                        begin x := a + i × h; f3 := f3 + fx end;
                        tn := (f3 + f2a + f1) × h; f2a := f2
                      end
              else begin for i := 1 step 2 until nn do begin x := a + i × h; f2 := f2 + fx end;
                        tn := (f2 + f1) × h
                      end
              end;
      extr(m); if abs(to - tr) ≤ ae + re × abs(tr) then goto end else to := tr
    end;
m := 0;
end: TRAPEX := tr
end TRAPEX;

real procedure INTEGRAND(a);
value a; real a;
begin real alp0, alpi, alpi1, eps, hsug, g, var, som1, som2;
integer i;
array INTAR[0:100];
alp0 := alp0 := ALPHANU(0); eps := alp0 × EPSFAKTOR × exp(-hnugedk/T);
hsug := 15/alp0; if hsug > RADIUS then hsug := RADIUS; hsug := hsug/100.001;
g := 0; INTAR[0] := BAR[0] × eps;
for i := 1 step 1 until 100 do
begin var := i × hsug;
alp1 := ALPHANU(var); eps := alp1 × EPSFAKTOR × exp(-hnugedk/T);
g := g + .5 × hsug × (alpi + alpi1);
INTAR[i] := B(g) × eps;
alpi := alpi1
end;
som1 := 0; som2 := 0;
for i := 1 step 2 until 99 do som1 := som1 + INTAR[i];
for i := 2 step 2 until 98 do som2 := som2 + INTAR[i];
INTEGRAND := hsug × (INTAR[0] + INTAR[100] + 4 × som1 + 2 × som2)/3
end INTEGRAND;

```

```

real procedure EPSILONU(R);
value R; real R;
begin EPSILONU := ALPHANU(R) * EPSFAKTOR * exp(-hnugedk/T);
end EPSILONU;

```

```

real procedure ALPHANU(R);
value R; real R;
begin RT(R, T);
    NU := NUO + a * BRO;
    ALPHANU := 2.86n+25 * Z2 * YAPPROX(nnu, alphau, betau, au, T)/(NU 3);
end ALPHANU;

```

```

procedure RT(R, T);
value R; real R, T;
begin integer og, mg, bg;
    og := 1; bg := RARMAX;
V:    mg := og + ((bg - og) : 2);
    if R < RAR[mg] then bg := mg else og := mg;
    if (bg - og) > 1.5 then goto V;
    T := (TRAR[bg] - TRAR[og]) * (R - RAR[og]) / (RAR[bg] - RAR[og]) + TRAR[og]
end RT;

```

```

real procedure B(g);
value g; real g;
begin integer og, mg, bg;
    if g > 15 then begin B := 0; goto eindbg end;
    og := 0; bg := 1500;
V:    mg := og + ((bg - og) : 2);
    if g < GAR[mg] then bg := mg else og := mg;
    if (bg - og) > 1.5 then goto V;
    B := (BAR[bg] - BAR[og]) * (g - GAR[og]) / (GAR[bg] - GAR[og]) + BAR[og];
end B;

```

```

real procedure EEN(a);
value a; real s;
begin NU:=NUO+a×BRO;
      hmgcdk:=h×NU/k; EPSFAKTOR:=2×h×NU×NU×NU/(c×c);
      EEN:=1
end EEN;
for I:=1 step 1 until MAX do
  begin TAR[I] := READ; UAR[I] := READ end;
  for I := 0 step 1 until 1500 do begin GAR[I] := READ; BAR[I] := READ end;
  for I:=1 step 1 until RARMAX do begin RAR[I]:=READ×n-3; TRAR[I]:=READ end;
  RADIUS:=RAR[RARMAX];
  ORTHOPOL(TAR UAR MAX nnu MAX-1 alphau betau au delta delta[nnu]/delta[-1]≤0-8);
  PRINTTEXT(⟨nnu=⟩); ABSFIXT(2,0,nnu); NLCR;
  PRINTTEXT(⟨radius=⟩); FLOT(5,3,RADIUS); NLCR;
  BRO := (NUMAX - NUO)/1000.001;
  pibro := 4 × pi × BRO;

begin integer amin,amax;
amin := 0; ANU := 0; ENU := 0;
NEW PAGE; e := 1;
for amax := 10, 100, 300, 1000 do
  begin ABSFIXT(3,0,LINE NUMBER);
        PRINTTEXT(⟨amin,amax m in anu en m in enu zijn achtereenvolgens=⟩);
        ABSFIXT(4,0,amin); ABSFIXT(4,0,amax);
        d := 2;
        ANU := ANU + TRAPEX(a, EEN(a) × ALPHANU(0) × INTEGRAND(a), amin, amax, 0, w-4, 10, TOP);
        ABSFIXT(3,0,ANU);
        d := 1;
        ENU := ENU + TRAPEX(a, EEN(a) × EPSILONU(0), amin, amax, 0, w-4, 10, TOP);
        ABSFIXT(3,0,ENU); NLCR;
        amin:=amax
  end;
  UNU := ENU - ANU; CARRIAGE(5);
  PRINTTEXT(⟨unu=⟩); FLOT(5,2,pibro×UNU); NLCR;
  PRINTTEXT(⟨anu=⟩); FLOT(5,2,pibro × ANU); NLCR;
  PRINTTEXT(⟨enu=⟩); FLOT(5,2,pibro×ENU);
  NLCR; PRINTTEXT(⟨unu is=⟩); FIXT(2,2,UNU/ENU×100); PRINTTEXT(⟨procent van enu=⟩);
end;
begin for I := 1 step 1 until e - 1 do UITVOER[3, I] := UITVOER[1, I] - UITVOER[2, I];
      CARRIAGE(5);
      PRINTTEXT(⟨ nu          enu          anu          unu=⟩); NLCR;
      for I := 1 step 1 until e - 1 do
        begin FLOT(5,2,NUO + (UITVOER[0, I] × BRO)); FLOT(5,3,UITVOER[1, I]);
              FLOT(5,3,UITVOER[2, I]); FLOT(5,3,UITVOER[3, I]); NLCR;
        end
      end;
end;
EIND;
end
progend

```